IEEE Access
Multidisciplinary | Rapid Review | Open Access Journal

Received 1 October 2022, accepted 27 October 2022, date of publication 1 November 2022, date of current version 8 November 2022.

Digital Object Identifier 10.1109/ACCESS.2022.3218721

RESEARCH ARTICLE

Downlink Analysis for the D2D Underlaid Multigroup Multicast Cell-Free Massive MIMO With Low-Resolution ADCs/DACs

JINWEN LI[1,2], ANPING WAN[1], MENG ZHOU[3,4], JIANTAO YUAN[3], (Member, IEEE), RUI YIN[3], (Senior Member, IEEE), AND LONGXIANG YANG[5]

[1]Department of Mechatronics Engineering, Zhejiang University City College, Hangzhou 310015, China
[2]College of Mechanical Engineering, Anhui University of Science and Technology, Huainan 232001, China
[3]School of Information and Electrical Engineering, Zhejiang University City College, Hangzhou 310015, China
[4]School of Information Science and Electronic Engineering, Zhejiang University, Hangzhou 310013, China
[5]Wireless Communication Key Laboratory of Jiangsu Province, Nanjing University of Posts and Telecommunications, Nanjing 210003, China

Corresponding author: Meng Zhou (zhoum2011@outlook.com)

This work was supported in part by the National Natural Science Foundation of China under Grant 61861039, Grant 62071246, and Grant 61427801; in part by the Jiangsu Provincial Key Research and Development Program under Grant BE20200845 and Grant BE20200841; and in part by the Science and Technology Project Foundation of Gansu Province under Grant 18YF1GA060.

ABSTRACT To fully utilize the scarce spectrum resources, the downlink device-to-device (D2D) underlaid multigroup multicast cell-free massive multi-input multi-output (MIMO) systems is proposed, where the geographically distributed access points (APs) serving both multi-antenna cell-free users (CFUEs) and D2D users (DUEs) pair over the same time/frequency resource blocks. Specially, the low-resolution analog-to-digital converters/digital-to-analog converters (ADCs/DACs) are adopted at the AP to effectively reduce hardware damage and energy costs. The imperfect channel state information (CSI) is obtained firstly by the standard minimum mean square error (MMSE), then the lower bounds of the closed-form achievable downlink rates for both CFUEs and DUEs are derived. Aside from that, the sum energy efficiency (EE) is also explored using the established power consumption model. Finally, numerical simulations are assessed to verify the analytical results and provide insights into the effects of the key system parameters. It demonstrates that increasing the number of APs can improve the sum SE, however, the sum EE decreases with the number of the APs sharply. Furthermore, increasing the density of DUEs can significantly improve the system capacity. The findings highlight the significance of the collaborative deployment of D2D and multigroup multicast cell-free massive MIMO technology, which can serve as a valuable reference and guide for the actual deployment of future communication systems.

INDEX TERMS Cell-free massive MIMO, D2D, energy efficiency, low-resolution ADCs/DACs, multigroup multicast, spectral efficiency.

I. INTRODUCTION

As a novel incarnation of centralized massive multi-input multi-output (MIMO) and distributed network MIMO, the advent of cell-free massive MIMO was yet pioneered in the groundbreaking contributions [1], [2]. In such systems, an enormous number of geographically distributed access points (APs) are deployed cooperatively communicating relative small users over the same time/frequency resource blocks and all APs have liaised with a central processing unit (CPU) via fronthaul links. It has been demonstrated that a five-fold gain in 95%-likely per-user throughput can be obtained when compared to the small cell scheme. Since it can potentially contribute multitudinous merits in terms of tremendous macroscopic diversity, coverage probability, ultrahigh spectral efficiency (SE), and energy efficiency (EE), it has

The associate editor coordinating the review of this manuscript and approving it for publication was Jad Nasreddine.

been consequently considered as one of the main building blocks toward the forthcoming beyond fifth-generation/sixth-generation (B5G/6G) projected to evolve [3], [4], [5], which has also been seriously triggered the growing research interest from the community of academic, industrial, and standardization bodies [4], [5], [6], [7].

Promoted by the above myriad benefits, the majority of recent research efforts have been focused on a roll [8], [9], [10], [11], [12], [13], [14]. The early works that relied on existing related contributions were mostly carried out within the specific context of the following techniques. For instance, a novel non-orthogonal multiple-access (NOMA) aided cell-free massive MIMO system was investigated in [8], [9], and [10] to meet the conflicting demands of high SE/EE/reliability and massive connectivity with low latency. Furthermore, as it can provide an outstanding capability of agilely moving in three-dimensional space, in [11] and [12] an unmanned aerial vehicle (UAV) enabled cell-free massive MIMO systems were considered for a wide-range of applications, which is able to remarkably relieve spatial limitations. Unlike traditional secrecy through cryptographic encryption, the authors in [13] and [14] use the trajectory design to tackle the physical layer security from an information-theoretic standpoint. To achieve the energy-efficient load balancing, in [15], the minimized total power consumption optimization was considered by jointly transmitting powers and hardware dissipation [16]. However, the works mentioned above only consider the general unicast transmissions.

Currently, the Global Internet Phenomena Report, released in January 2022, indicates that accounting for 53.72 percent of the entire Internet is primarily dominated by multicast applications, such as video conferencing, software updates, and streaming media, in the daily routines and shows a trend of explosive growth [17]. However, the increasing demand places a significant strain due to the scarcity and insufficient the available radio spectrum resource, which has become a major factor limiting the system performance and making it difficult to provide the users with the expected quality of experience (QoE) provisioning as well. These enormous drivers have inspired generous research efforts toward efficient spectrum utilization.

A. BACKGROUND AND MOTIVATION

As an effective way of allowing multiple multicast contents to deliver to various groups simultaneously, multicast multigroup transmission has triggered rapid advances in full swing since it can efficaciously relieve the pressure of ultrahigh volumes of network traffic in conventional systems and it is a consensus that will play a pivotal role in the forthcoming system. In reality, multigroup multicast named as evolved multimedia broadcast/multicasting service (eMBMS) has been incorporated into the third-Generation Partnership Project (3GPP) Release-17 [18]. For this, the literature [19] analyzed the performance of multicast multigroup cell-free massive MIMO systems by using the distributed conjugate beamforming (CB) precoder with the short-term power constraint. It demonstrates that the larger group number or higher Eve's spoofing pilot power leads to significant degradation of secrecy performance. On this basis, the work [20] further investigated the physical layer security performance in the presence of pilot spoofing attack, and [21] explored the effects of multiantenna users and low-resolution analog-to-digital converters/digital-to-analog converters (ADCs/DACs) on multigroup multicast downlink cell-free massive MIMO systems. It reveals that substituting 5-bit DACs for full-resolution can achieve the same performance, and when DAC quantization is equal to 2-bit, the maximum sum EE can be achieved. By taking the effects of channel estimation, pilot contamination, and different precoding schemes into account, a joint unicast and multigroup multicast cell-free massive MIMO was studied in [22], proving the proposed architecture can effectively achieve the higher SE.

In parallel, as a compelling candidate enabler that allows direct transmission between devices located in close proximity, device-to-device (D2D) is continuously evolving and engulfing a wide diversity of intensive applications, which has been considered as one of the pivotal technologies to making more efficient use of spectrum resources and was originally conceived for long term evolution-advanced (LTE-A) under the 3GPP Release-12 [23], [24], [25]. With all the benefits listed above, D2D proposes a new epitome to take full advantage of the proximity of users for efficient utilization of available resources, features of D2D could be explored to shed light on the potential of offloading wireless traffic, reducing transmission latency, corroborating proximity-based services, extending the battery life of users, and upgrading SE/EE. Inspired by the preceding consideration, various research communities around have been intensively exploring the potential techniques of the D2D underlaid paradigm to enable its seamless integration with the B5G/6G. In academia, D2D communication was first proposed in [26] to enable multihop relays in cellular networks. Later, the research in [27] looked into the potential of D2D communication for improving the SE of cellular networks. For the traditional massive MIMO systems, the works [28], [29], and [30] examined the interaction between the traditional massive MIMO systems and underlay D2D communication.

The work [31] first studied the coexistence of D2D and cell-free massive MIMO uplink systems with low-resolution ADC. It shows that activating D2D links has a positive impact on SE. Besides, by assuming imperfect CSI is available in [32], we considered a D2D underlaid downlink cell-free massive MIMO system. To maximize the average sum rate, a path-following algorithm was proposed.

B. CONTRIBUTIONS AND OUTCOMES

To the best of the authors' knowledge, the amalgamation of these two disjoint networking techniques, known as multigroup multicast cell-free massive MIMO and D2D communication, has not received further attention by the research

academic, particularly for the regimes of multiantenna both at APs and users.

Promoted by the preceding consideration, in this paper, the novelty and specific contribution are summarized as follows.

1) Assuming that the imperfect CSI is available, the estimated channel properties of both two links are derived by using the general minimum mean square error (MMSE) technique, which is paimarily used for multiplexing in the sequence.
2) With the CB precoder and maximal ratio transmission (MRT), the closed-form achievable rate for both cell-free users (CFUEs) and D2D users (DUEs) are calculated, respectively. After performing the capacity bounding technique and several analyses, some significant insights are attained with the derived results.
3) Based on the established power consumption model and the derived sum rates, a system-level sum EE is then derived. Finally, numerical simulations are provided to enable us to give insights into the effects of the key system parameters. It shows that increasing the number of APs can improve the sum SE, however, the sum EE decreases as the number of the APs increases.

C. ORGANIZATION AND NOTATIONS

Organization: The remainder of this paper is briefly organized as follows. The considered D2D underlaid multigroup multicast cell-free massive MIMO model is described in Section II and the analysis methodology of achievable rate is conducted in Section III. Then the sum-EE is performed based on the established system-level power cost model in Section IV. Moreover, the main derived results and derivations are presented in Section V which is further supported by numerical simulations. Finally, we draw out our concluding remarks in Section VI and prove our various claims in the Appendices.

Notation: For notational simplicity, we mention the common notations used in this article. Boldface uppercase $\mathbf{X}$ and lowercase $\mathbf{x}$ are denoted matrices and vectors. The superscripts $(.)^T$, $(.)^*$, $(.)^{-1}$, and $(.)^H$ represent the transpose, conjugate, inverse, and conjugate transpose, respectively. The symbol $\mathbb{E}\{.\}$ stands for the statistical expectation operator. Likewise, the shorthand notation $\mathbf{n} \sim \mathcal{CN}\left(0, \sigma^2\right)$ denotes that the random vector $\mathbf{n}$ follows a zero-mean circularly symmetric complex Gaussian distribution with covariance matrix σ^2.

II. SYSTEM MODEL AND PRELIMINARIES

In this paper, the D2D underlaid multigroup multicast cell-free massive MIMO model is outlined as shown in Fig. 1, where M geographically distributed APs over a large area to serve $J \times K$ multi-antenna CFUEs and L DUEs pair in the same time/frequency resource blocks,[1] $M \geq J$. Besides,

[1]In attention, all JK CFUEs are equally scattered into J groups and each CFUE only listens to a single group.

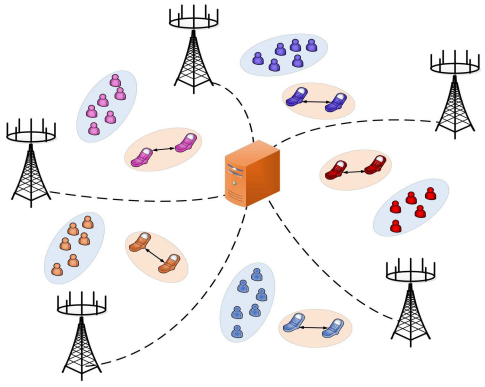

FIGURE 1. D2D underlaid multigroup multicast cell-free massive MIMO model.

each AP, CFUE, and DUE has N_{A}, N, and N_{D} antennas, respectively. As presumed in [1], all APs are coordinated and connected to a CPU via an ideal backhaul link with error-free and infinite capacity.

A. CHANNEL MODEL

For sake of analysis, the wireless channel is assumed to experience quasi-static Rayleigh block fading [1], [4], [13], [21], [32]. That is, the fading coefficients remain constant during each transmission slot and change independently from one to another.

Assuming that the uncorrelated Rayleigh channel is used, we denote $\mathbf{G}^{\mathrm{a}}_{mjk} \in {}^{N_{\mathrm{A}} \times N}$ as the channel response from the mth AP to the kth CFUE in the jth group, which can be modelled as [33]

$$\mathbf{G}^{\mathrm{a}}_{mjk} = \beta^{1/2}_{mjk}\mathbf{H}_{mjk}, \tag{1}$$

where $\beta_{mjk}, \forall m, \forall j, \forall k$ accounts for the large-scale fading (LSF) factor associated with path loss and shadow fading, and $\mathbf{H}_{mjk}$ captures the small-scale fading (SSF) matrix whose entries are independent and identically distributed (i.i.d.) random variables, according to (0, 1).

Subsequently, for the lth D2D pairs, the channel matrix between the DUE transmitter $\mathrm{DUE}^{\mathrm{Tx}}_{l'}$ and the receiver $\mathrm{DUE}^{\mathrm{Rx}}_{l}$, $\mathbf{G}^{\mathrm{d}}_{ll'} \in \mathbb{C}^{N_{\mathrm{D}} \times N_{\mathrm{D}}}$ can be given as follows

$$\mathbf{G}^{\mathrm{d}}_{ll'} = \beta^{1/2}_{ll'}\mathbf{H}_{ll'}, \tag{2}$$

where $\beta_{ll'}$ stands for the LSF and the elements of random matrix, $\mathbf{H}_{ll'}$ of Rayleigh distribution denotes i.i.d. random variables $[\mathbf{H}_{ll'}]_{mn} \sim \mathcal{CN}(0, 1)$, [31], [32].

B. MMSE CHANNEL ESTIMATION

During the uplink training phase, the time division duplexing (TDD) mode is adopted. By exploiting the channel reciprocity, the downlink channel is typically obtained via estimating the uplink channel, which can be exploited to facilitate adaptive transmission for improving the system performance, without incurring a feedback overhead penalty. During the τ_{c}-length coherence interval, the τ_{p}-length orthogonal pilot sequences $\mathbf{\Xi} \in \mathbb{C}^{\tau_{\mathrm{p}} \times \tau_{\mathrm{p}}}$ are allowed with $\mathbf{\Xi}^H\mathbf{\Xi} = \mathbf{I}_{\tau_{\mathrm{p}}}$,

$\tau_{\mathrm{p}} \geq K + LN_{\mathrm{D}}$. Here, the pilot sequence set used by CFUEs and DUEs are respectively given as $\boldsymbol{\Phi} \in \boldsymbol{\Xi}$ and $\boldsymbol{\Omega} \subset \boldsymbol{\Xi}$. Then the assigned pilots of CFUE_k and $\mathrm{DUE}_{l'}^{\mathrm{Tx}}$ are expressed $\boldsymbol{\Phi}_j \in \mathbb{C}^{\tau_{\mathrm{p}} \times N}$ and $\boldsymbol{\Omega}_l \in \mathbb{C}^{\tau_{\mathrm{p}} \times N_{\mathrm{D}}}$.

1) FOR THE AP TO CFUE CHANNEL

To effectively reduce the limited pilot resource overhead, it is assumed that the same pilot sequence is assigned within each group of users as [19], [20], and [21]. Then, the received pilot signal at the mth AP is given as

$$\mathbf{Y}_{\mathrm{p},m}^{\mathrm{a}} = \sqrt{\tau_{\mathrm{p}}\rho_{\mathrm{p}}^{\mathrm{c}}} \sum_{j=1}^{J}\sum_{k=1}^{K} \mathbf{G}_{mjk}^{\mathrm{a}} \boldsymbol{\Phi}_j^H + \sqrt{\tau_{\mathrm{p}}\rho_{\mathrm{p}}^{\mathrm{d}}} \sum_{l'=1}^{L} \mathbf{G}_{ml'}^{\mathrm{a}} \boldsymbol{\Omega}_{l'}^H + \mathbf{W}_{\mathrm{p},m}^{\mathrm{a}}, \tag{3}$$

where $\rho_{\mathrm{p}}^{\mathrm{c}}$ and $\rho_{\mathrm{p}}^{\mathrm{d}}$ model the corresponding normalized signal-to-noise ratio (SNR) of CFUE_k and $\mathrm{DUE}_{l'}^{\mathrm{Tx}}$, respectively. Besides, $\mathbf{G}_{ml'} \in \mathbb{C}^{N_{\mathrm{A}} \times N_{\mathrm{D}}}$ and $\mathbf{W}_{\mathrm{p},m}^{\mathrm{a}} \in \mathbb{C}^{N_{\mathrm{A}} \times \tau_{\mathrm{p}}}$ characterize the transmission channel from mth AP to l'th $\mathrm{DUE}_{l'}^{\mathrm{Rx}}$, and the additive white Gaussian noise (AWGN) at the mth AP.

Likewise, the received pilot signals at the $\mathrm{DUE}_l^{\mathrm{Rx}}$ are as follows

$$\mathbf{Y}_{\mathrm{p},l}^{\mathrm{d}} = \sqrt{\tau_{\mathrm{p}}\rho_{\mathrm{p}}^{\mathrm{c}}} \sum_{j=1}^{J}\sum_{k=1}^{K} \mathbf{G}_{lk}^{\mathrm{d}} \boldsymbol{\Phi}_j^H + \sqrt{\tau_{\mathrm{p}}\rho_{\mathrm{p}}^{\mathrm{d}}} \sum_{l'=1}^{L} \mathbf{G}_{ll'}^{\mathrm{d}} \boldsymbol{\Omega}_{l'}^H + \mathbf{W}_{\mathrm{p},l}^{\mathrm{d}}, \tag{4}$$

where the entries of AWGN $\mathbf{W}_{\mathrm{p},l}^{\mathrm{d}}$ are i.i.d. random variables as well, and $\mathbf{G}_{lk}^{\mathrm{d}} \in \mathbb{C}^{N_{\mathrm{D}} \times N}$ denotes the transmit channel for DUEs communication link.

Following the execution of the dispreading operation, in the following, the processed signal can be represented as [34]

$$\begin{aligned}\mathbf{Y}_{\mathrm{p},mj}^{\mathrm{a}} &\triangleq \mathbf{Y}_{\mathrm{p},m}^{\mathrm{a}} \boldsymbol{\Phi}_j \\ &= \sqrt{\tau_{\mathrm{p}}\rho_{\mathrm{p}}^{\mathrm{c}}} \sum_{j'=1}^{J}\sum_{k'=1}^{K} \mathbf{G}_{mj'k'}^{\mathrm{a}} \boldsymbol{\Phi}_{j'}^H \boldsymbol{\Phi}_j + \sqrt{\tau_{\mathrm{p}}\rho_{\mathrm{p}}^{\mathrm{d}}} \sum_{l'=1}^{L} \mathbf{G}_{ml'}^{\mathrm{a}} \boldsymbol{\Omega}_{l'}^H \boldsymbol{\Phi}_j + \mathbf{W}_{\mathrm{p},m}^{\mathrm{a}} \boldsymbol{\Phi}_j \\ &= \sqrt{\tau_{\mathrm{p}}\rho_{\mathrm{p}}^{\mathrm{c}}} \sum_{j'=1}^{J}\sum_{k'=1}^{K} \mathbf{G}_{mj'k'}^{\mathrm{a}} \boldsymbol{\Phi}_{j'}^H \boldsymbol{\Phi}_j + \widetilde{\mathbf{W}}_{\mathrm{p},mj},\end{aligned} \tag{5}$$

where $\widetilde{\mathbf{W}}_{\mathrm{p},mj} \triangleq \mathbf{W}_{\mathrm{p},m}^{\mathrm{a}} \boldsymbol{\Phi}_j$ is composed of $N_{\mathrm{A}} \times N$ i.i.d. components. Besides, assuming $\boldsymbol{\Omega}_{l'}^H \boldsymbol{\Phi}_j = \mathbf{0}$ for eliminating the pilot coupling [31], [32].

Considering the huge hardware costs and energy consumption at AP, in this paper, the low-resolution ADCs are deployed as [6], [21], and [32]. For simplicity, the general additive quantization noise model (AQNM) is performed. Based on the received pilot signal, after quantization, the received pilot signal at mth AP can be further expressed as

$$\begin{aligned}\widetilde{\mathbf{Y}}_{\mathrm{p},mj}^{\mathrm{a}} &= \lambda_m \mathbf{Y}_{\mathrm{p},mj}^{\mathrm{a}} + \widetilde{\mathbf{W}}_{\mathrm{p},m} \\ &= \lambda_m \sqrt{\tau_{\mathrm{p}}\rho_{\mathrm{p}}^{\mathrm{c}}} \sum_{j=1}^{J}\sum_{k=1}^{K} \mathbf{G}_{mjk}^{\mathrm{a}} \boldsymbol{\Phi}_{j'}^H \boldsymbol{\Phi}_j + \lambda_m \widetilde{\mathbf{W}}_{\mathrm{p},mj} + \widetilde{\mathbf{W}}_{\mathrm{p},m},\end{aligned} \tag{6}$$

where $\lambda_m, \forall m$ represents the linear gain associated with the quantization bits b_m^{ADC}, and the covariance of the additive Gaussian quantization noise matrix $\widetilde{\mathbf{W}}_{\mathrm{p},m}$ can be written as

$$\begin{aligned}R_{\widetilde{\mathbf{W}}_{\mathrm{p},m}} &\triangleq \lambda_m (1-\lambda_m) \operatorname{diag}\left(\left\{\mathbf{Y}_{\mathrm{p},mj}^{\mathrm{a}} \left(\mathbf{Y}_{\mathrm{p},mj}^{\mathrm{a}}\right)^H\right\}\right) \\ &= N_{\mathrm{A}} \lambda_m (1-\lambda_m) \\ &\quad \times \left(\tau_{\mathrm{p}}\rho_{\mathrm{p}}^{\mathrm{c}} \sum_{j'=1}^{J}\sum_{k'=1}^{K} \beta_{mj'k'} \left\|\boldsymbol{\Phi}_{j'}^H \boldsymbol{\Phi}_j\right\|^2 + \mathbf{I}_{\tau_{\mathrm{p}}}\right).\end{aligned} \tag{7}$$

Theorem 1: Following the MMSE, the estimated channel response $\widehat{\mathbf{G}}_{mjk}^{\mathrm{a}}$ can be expressed as [35]

$$\widehat{\mathbf{G}}_{mjk}^{\mathrm{a}} = \frac{\sqrt{\tau_{\mathrm{p}}\rho_{\mathrm{p}}^{\mathrm{c}}}\beta_{mjk}}{\tau_{\mathrm{p}}\rho_{\mathrm{p}}^{\mathrm{c}} \sum_{j'=1}^{J}\sum_{k'=1}^{K} \beta_{mjk'} \left\|\boldsymbol{\Phi}_{j'}^H \boldsymbol{\Phi}_j\right\|^2 + \mathbf{I}_N} \widetilde{\mathbf{Y}}_{\mathrm{p},mj}^{\mathrm{a}}, \tag{8}$$

where $\mathbf{G}_{mjk} = \widehat{\mathbf{G}}_{mjk} + \mathbf{E}_{mjk}$, in which $\mathbf{E}_{mjk}$ denotes the channel estimation error.

For notational compactness, the covariance of the entries of term $\widehat{\mathbf{G}}_{mjk}^{\mathrm{a}}$ can be accordingly given by, mathematically

$$\gamma_{mjk} \triangleq \mathbb{E}\left\{\left|\left[\widehat{\mathbf{G}}_{mjk}^{\mathrm{a}}\right]_{m,n}\right|^2\right\} = \frac{\lambda_m \tau_{\mathrm{p}}\rho_{\mathrm{p}}^{\mathrm{c}}\beta_{mjk}^2}{\tau_{\mathrm{p}}\rho_{\mathrm{p}}^{\mathrm{c}} \sum_{k'=1}^{K} \beta_{mjk'} + 1}. \tag{9}$$

With reference to [19] and [21], as such, in principle the estimated matrix $\widehat{\mathbf{G}}_{mjk}^{\mathrm{a}}$ can be re-expressed as

$$\widehat{\mathbf{G}}_{mjk}^{\mathrm{a}} \triangleq \gamma_{mjk}^{1/2} \mathbf{Z}_{mj}^{\mathrm{a}}, \tag{10}$$

where $\mathbf{Z}_{mj}^{\mathrm{a}}$ stands for the beamforming matrix which can be expressed as $\left[\mathbf{Z}_{mj}^{\mathrm{a}}\right]_N \sim \mathcal{CN}\left(0, \mathbf{I}_{N_{\mathrm{A}}}\right)$.

Proof 1: See Appendix A.

2) FOR THE DUE TO DUE CHANNEL

Without loss of generality, for D2D links, $\mathrm{DUE}_l^{\mathrm{Rx}}$ performs despreading operation to estimate $\mathbf{G}_{ll'}$, which can be re-written as

$$\widetilde{\mathbf{Y}}_{\mathrm{p},ll}^{\mathrm{d}} \triangleq \mathbf{Y}_{\mathrm{p},l}^{\mathrm{d}} \boldsymbol{\Omega}_l = \sqrt{\tau_{\mathrm{p}}\rho_{\mathrm{p}}^{\mathrm{d}}} \sum_{l'=1}^{L} \mathbf{G}_{ll'}^{\mathrm{d}} \boldsymbol{\Omega}_{l'l} + \mathbf{W}_{\mathrm{p},l}^{\mathrm{d}} \boldsymbol{\Omega}_l, \tag{11}$$

where $\boldsymbol{\Omega}_{l'l}$ is defined as $\boldsymbol{\Omega}_{l'l} \triangleq \boldsymbol{\Omega}_{l'}^H \boldsymbol{\Omega}_l$.

Guided by the above consideration as Theorem 1, consequently, the estimated D2D channel matrix $\widehat{\mathbf{G}}_{ll'}^{\mathrm{d}}$ can be expressed as

$$\widehat{\mathbf{G}}_{ll'}^{\mathrm{d}} = \widetilde{\mathbf{Y}}_{\mathrm{p},ll'}^{\mathrm{d}} \mathbf{C}_{ll'}, \tag{12}$$

where $\mathbf{C}_{ll}$ is specified as

$$\mathbf{C}_{ll'} = \frac{\sqrt{\tau_{\mathrm{p}}\rho_{\mathrm{p}}^{\mathrm{d}}}\beta_{ll}^{\mathrm{d}}}{\tau_{\mathrm{p}}\rho_{\mathrm{p}}^{\mathrm{d}}\sum\limits_{l'=1}^{L}\beta_{ll'}^{\mathrm{d}}\mathbf{\Omega}_{l'l}^{H}\mathbf{\Omega}_{l'l}+\mathbf{I}_{N_{\mathrm{D}}}}. \tag{13}$$

C. DOWNLINK DATA TRANSMISSION

In this phase, we consider implementing the linear CB precoder at AP to separate the signals sent by multiple users thanks to its implementation simplicity. Then the emitted signal at the mth AP is given as [1], [2],

$$\mathbf{x}_m^{\mathrm{a}} = \sqrt{\rho^{\mathrm{a}}}\sum_{j=1}^{J}\sum_{k=1}^{K}\eta_{mjk}^{1/2}\mathbf{Z}_{mj}^{\mathrm{a}}\mathbf{q}_j, \tag{16}$$

where ρ^{a} stands for the maximum transmitted power of AP, η_{mjk} denotes the power distribution coefficient, and $\mathbf{q}_j$ represents the desired independent multicast Gaussian signal for the jth multicast group, which following $\mathbb{E}\left\{\mathbf{q}_j\mathbf{q}_j^H\right\} = \mathbf{I}_N$.

To elaborate on the signal processing at the AP and considering the fact that the low-resolution DACs are deployed, by virtue of (16), the quantized signal after processing is given as

$$\begin{aligned}\widetilde{\mathbf{x}}_m^{\mathrm{a}} &= \alpha_m\mathbf{x}_m^{\mathrm{a}} + \tilde{\mathbf{n}}_m \\ &= \sqrt{\rho^{\mathrm{a}}}\alpha_m\sum_{j=1}^{J}\sum_{k=1}^{K}\eta_{mjk}^{1/2}\mathbf{Z}_{mj}^{\mathrm{a}}\mathbf{q}_j + \tilde{\mathbf{n}}_m,\end{aligned} \tag{17}$$

where α_m refers to the linear gain decided by the quantification bits b_m^{DAC} and $\tilde{\mathbf{n}}_m$ describes the additive Gaussian quantization noise. Furthermore, α_m and $\tilde{\mathbf{n}}_m$ are independent of each other and $\tilde{\mathbf{n}}_m$ follows Gaussian-distribution with zero means [31] and [32].

Referring to the derivation process as [7] and [36], the covariance matrix of $\tilde{\mathbf{n}}_m$ can be denoted by

$$\begin{aligned}R_{\tilde{\mathbf{n}}_m} &\triangleq \alpha_m(1-\alpha_m)\,\mathrm{diag}\left(\mathbb{E}\left\{\mathbf{x}_m^{\mathrm{a}}\left(\mathbf{x}_m^{\mathrm{a}}\right)^H\right\}\right) \\ &= N\rho^{\mathrm{a}}\alpha_m(1-\alpha_m)\sum_{j=1}^{J}\left(\sum_{k=1}^{K}\eta_{mjk}^{1/2}\right)^2\mathbf{I}_{N_{\mathrm{A}}}.\end{aligned} \tag{18}$$

To meet the power constraint of each AP, i.e., $\mathbb{E}\left\{\left\|\widetilde{\mathbf{x}}_m^{\mathrm{a}}\right\|^2\right\} \le \rho^{\mathrm{a}}$, the power constraint can be written as

$$\begin{aligned}\mathbb{E}\left\{\left\|\widetilde{\mathbf{x}}_m^{\mathrm{a}}\right\|^2\right\} &= N_{\mathrm{A}}N\rho^{\mathrm{a}}\alpha_m^2\sum_{j=1}^{J}\left(\sum_{k=1}^{K}\eta_{mjk}^{1/2}\right)^2 \\ &\quad + N_{\mathrm{A}}N\rho^{\mathrm{a}}\alpha_m(1-\alpha_m)\sum_{j=1}^{J}\left(\sum_{k=1}^{K}\eta_{mjk}^{1/2}\right)^2 \\ &= N_{\mathrm{A}}N\rho^{\mathrm{a}}\alpha_m\sum_{j=1}^{J}\left(\sum_{k=1}^{K}\eta_{mjk}^{1/2}\right)^2.\end{aligned} \tag{19}$$

Using these notations and further simplifying, we can obtain

$$\sum_{j=1}^{J}\left(\sum_{k=1}^{K}\eta_{mjk}^{1/2}\right)^2 \le \frac{1}{\alpha_m N_{\mathrm{A}}N}. \tag{20}$$

For the D2D links, similarly, it is assumed that the MRT precoder is used in $\mathrm{DUE}_l^{\mathrm{Tx}}$, the emitted signal $\mathbf{x}_l^{\mathrm{d}}$ is also given by [16], [28]

$$\mathbf{x}_l^{\mathrm{d}} = \sqrt{\rho^{\mathrm{d}}u_l}\widehat{\mathbf{G}}_{ll}^{\mathrm{d}}\mathbf{s}_l, \tag{21}$$

where ρ^{d} is the maximum SNR of the lth DUE transmitter, u_l denotes the power allocation coefficient, and $\mathbf{s}_l$ represents the desired Gaussian signal for the lth DUE receiver, which following $\mathbb{E}\left\{\mathbf{s}_l\mathbf{s}_l^H\right\} = \mathbf{I}_{N_{\mathrm{D}}}$. To satisfy the power constraint of each DUE, $\mathbb{E}\left\{\left\|\mathbf{x}_l^{\mathrm{d}}\right\|^2\right\} \le \rho^{\mathrm{d}}$, it can be rewritten as

$$\begin{aligned}\mathbb{E}\left\{\left\|\mathbf{x}_l^{\mathrm{d}}\right\|^2\right\} &= \rho^{\mathrm{d}}u_l\mathbb{E}\left\{\tau_{\mathrm{p}}\rho_{\mathrm{p}}^{\mathrm{d}}\left(\beta_{ll}^{\mathrm{d}}\right)^2\mathbf{\Omega}_{l'l}\mathbf{C}_{ll}\mathbf{C}_{ll}^H\mathbf{\Omega}_{l'l}^H\right\} \\ &= \rho^{\mathrm{d}}N_{\mathrm{D}}u_l\,\mathrm{tr}\left(\mathbf{\Gamma}_{ll}\right),\end{aligned} \tag{22}$$

where $\mathbf{\Gamma}_{ll}$ can be expressed as

$$\mathbf{\Gamma}_{ll} \triangleq \sqrt{\tau_{\mathrm{p}}\rho_{\mathrm{p}}^{\mathrm{d}}}\beta_{ll}^{\mathrm{d}}\mathbf{C}_{ll'}. \tag{23}$$

Therefore, we have

$$\mathrm{tr}\left(\mathbf{\Gamma}_{ll}\right) \le \frac{1}{\mu_l N_{\mathrm{D}}}. \tag{24}$$

Mathematically, the received signal for the kth CFUE in the jth group can be given by [29]

$$\mathbf{r}_{jk}^{\mathrm{c}} = \sum_{m=1}^{M}\left(\mathbf{G}_{mjk}^{\mathrm{a}}\right)^H\widetilde{\mathbf{x}}_m^{\mathrm{a}} + \sum_{l=1}^{L}\left(\mathbf{G}_{lk}^{\mathrm{d}}\right)^H\mathbf{x}_l^{\mathrm{d}} + \mathbf{n}_{jk}, \tag{25}$$

$$R_{jk}^{\mathrm{c}} = N\log_2\left(1 + \frac{\left(N_{\mathrm{A}}\sqrt{\rho_{\mathrm{d}}^{\mathrm{a}}}\sum\limits_{m=1}^{M}\sum\limits_{k'=1}^{K}\eta_{mj'k'}^{1/2}\gamma_{mjk}^{1/2}\right)^2}{\rho_{\mathrm{d}}^{\mathrm{a}}NN_{\mathrm{A}}\sum\limits_{m=1}^{M}\sum\limits_{k'=1}^{K}\sum\limits_{k''=1}^{K}\alpha_m^2\beta_{mjk}\eta_{mjk'}^{1/2}\eta_{mjk''}^{1/2} + \mathbf{\Theta}_{mj} + N_{\mathrm{D}}^2\sum\limits_{l=1}^{L}\mu_l\beta_{lk}^{\mathrm{d}}\,\mathrm{tr}\left(\mathbf{\Gamma}_{ll}\right) + 1}\right), \tag{14}$$

$$\mathbf{\Theta}_{mj} = \rho_{\mathrm{d}}^{\mathrm{a}}NN_{\mathrm{A}}\sum_{m=1}^{M}\sum_{j=1}^{J}\alpha_m(1-\alpha_m)\beta_{mjk}\left(\sum_{k'=1}^{K}\eta_{mjk'}^{1/2}\right)^2 - \left(N_{\mathrm{A}}\sqrt{\rho_{\mathrm{d}}^{\mathrm{a}}}\sum_{m=1}^{M}\sum_{k'=1}^{K}\alpha_m\eta_{mjk'}^{1/2}\gamma_{mjk}^{1/2}\right)^2. \tag{15}$$

where $\mathbf{n}_{jk}$ indicates the AWGN satisfying $\mathbf{n}_{jk} \sim \mathcal{CN}(\mathbf{0}, \mathbf{I}_N)$.

Guided by the preceding consideration, the received signal at lth receiver $\mathrm{DUE}_l^{\mathrm{Rx}}$ is formulated as

$$\mathbf{r}_l^{\mathrm{d}} = \sum_{m=1}^{M} \left(\mathbf{G}_{ml}^{\mathrm{a}}\right)^H \widetilde{\mathbf{x}}_m^{\mathrm{a}} + \sum_{l'=1}^{L} \left(\mathbf{G}_{l'l}^{\mathrm{d}}\right)^H \mathbf{x}_{l'}^{\mathrm{d}} + \mathbf{n}_l, \tag{26}$$

where $\mathbf{n}_l$ is additive noise, $\mathbf{n}_l \sim \mathcal{CN}\left(\mathbf{0}, \mathbf{I}_{N_{\mathrm{D}}}\right)$.

III. ANALYSIS METHODOLOGY OF ACHIEVABLE RATE

Based on the preceding evolution, in this section, the expected rate analysis of both CFUEs and DUEs is performed as follows, which primarily through the use of a general bounding technique [19], [37].

A. ACHIEVABLE DOWNLINK RATE OF CFUEs

Based on the derived results as (17) and (25), it can be rewritten as

$$\begin{aligned}\mathbf{r}_{jk}^{\mathrm{c}} = & \underbrace{\sqrt{\rho^{\mathrm{a}}} \sum_{m=1}^{M}\sum_{j=1}^{J}\sum_{k=1}^{K} \alpha_m \eta_{mjk}^{1/2} \left(\mathbf{G}_{mjk}^{\mathrm{a}}\right)^H \mathbf{Z}_{mj}^{\mathrm{a}} \mathbf{q}_j}_{\mathbf{H}_{jk}} \\ & + \sqrt{\rho^{\mathrm{d}}} \sum_{l=1}^{L} \sqrt{u_l} \left(\mathbf{G}_{lk}^{\mathrm{d}}\right)^H \widehat{\mathbf{G}}_{ll}^{\mathrm{d}} \mathbf{s}_l \\ & + \sum_{m=1}^{M} \left(\mathbf{G}_{mjk}^{\mathrm{a}}\right)^H \tilde{\mathbf{n}}_m + \mathbf{n}_{jk}. \end{aligned} \tag{29}$$

Capitalizing on the received signal $\mathbf{r}_{jk}^{\mathrm{c}}$ and side information $\bar{\mathbf{H}}_{jk}$ [19], [21], [26], [32], [38], the achievable downlink rate of kth CFUE in the jth group can be obtained as

$$R_{jk}^{\mathrm{c}} = \log_2 \left| \mathbf{I}_N + \bar{\mathbf{H}}_{jk}^H \left(\bar{\mathbf{\Psi}}_{jk}^{\mathrm{c}}\right)^{-1} \bar{\mathbf{H}}_{jk} \right|, \tag{30}$$

where $\bar{\mathbf{H}}_{jk}$ and $\bar{\mathbf{\Psi}}_{jk}^{\mathrm{c}}$ can be respectively denoted by

$$\bar{\mathbf{H}}_{jk} \triangleq \mathbb{E}\left\{\mathbf{H}_{jk}\right\} = \mathbb{E}\left\{ \sqrt{\rho_{\mathrm{d}}^{\mathrm{a}}} \sum_{m=1}^{M}\sum_{k'=1}^{K} \alpha_m \eta_{mjk'}^{1/2} \mathbf{G}_{mjk}^{\mathrm{a}} \mathbf{Z}_{mj}^{\mathrm{a}} \right\}, \tag{31}$$

and

$$\begin{aligned}\bar{\mathbf{\Psi}}_{jk}^{\mathrm{c}} \triangleq \mathbb{E}\Bigg\{ & \rho_{\mathrm{d}}^{\mathrm{a}} \sum_{m=1}^{M}\sum_{n=1}^{N}\sum_{j'=1}^{J}\sum_{k'=1}^{K}\sum_{k''=1}^{K} \alpha_m \alpha_n \eta_{mj'k'}^{1/2} \eta_{njk''}^{1/2} \\ & \times \left(\mathbf{G}_{mjk}^{\mathrm{a}}\right)^H \mathbf{Z}_{mj'}^{\mathrm{a}} \left(\mathbf{Z}_{nj'}^{\mathrm{a}}\right)^H \mathbf{G}_{njk}^{\mathrm{a}} + \mathbf{I}_N \\ & + \rho^{\mathrm{d}} \sum_{l=1}^{L} \mu_l \left(\mathbf{G}_{lk}^{\mathrm{d}}\right)^H \widehat{\mathbf{G}}_{ll}^{\mathrm{d}} \left(\widehat{\mathbf{G}}_{ll}^{\mathrm{d}}\right)^H \mathbf{G}_{lk}^{\mathrm{d}} \\ & + \sum_{m=1}^{M} \left(\mathbf{G}_{mjk}^{\mathrm{a}}\right)^H \tilde{\mathbf{n}}_m \tilde{\mathbf{n}}_m^H \mathbf{G}_{mjk}^{\mathrm{a}} - \bar{\mathbf{H}}_{jk} \bar{\mathbf{H}}_{jk}^H \Bigg\}. \end{aligned} \tag{32}$$

Theorem 2: Using the central-limit theorem and capacity bounding technique from [1] and [10], in the following, we give the lower bound on the achievable rate for the kth CFUE in the jth group by skipping tedious derivation which can be given as (14), shown at the bottom of the previous page.

Proof 2: See Appendix B.

B. ACHIEVABLE DOWNLINK RATE OF DUEs

With the preceding in mind, the received signal $\mathbf{r}_l^{\mathrm{d}}$ in (26) can be rewritten as [38]

$$\begin{aligned}\mathbf{r}_l^{\mathrm{d}} = & \underbrace{\sqrt{\rho^{\mathrm{d}}} \sum_{l'=1}^{L} \sqrt{\mu_{l'}} \left(\mathbf{G}_{l'l}^{\mathrm{d}}\right)^H \widehat{\mathbf{G}}_{l'l'}^{\mathrm{d}} \mathbf{q}_{l'}}_{\mathbf{S}_{l'l'}} \\ & + \sqrt{\rho^{\mathrm{a}}} \sum_{m=1}^{M}\sum_{j=1}^{J}\sum_{k=1}^{K} \alpha_m \eta_{mjk}^{1/2} \left(\mathbf{G}_{ml}^{\mathrm{a}}\right)^H \mathbf{Z}_{mj}^{\mathrm{a}} \mathbf{q}_j \\ & + \sum_{m=1}^{M} \left(\mathbf{G}_{ml}^{\mathrm{a}}\right)^H \tilde{\mathbf{n}}_m + \mathbf{n}_l. \end{aligned} \tag{34}$$

As a result, the achievable downlink rate of lth DUE receiver is given by

$$R_l^{\mathrm{d}} = \log_2 \left| \mathbf{I}_{N_{\mathrm{D}}} + \bar{\mathbf{S}}_{ll}^H \left(\bar{\mathbf{\Psi}}_l^{\mathrm{d}}\right)^{-1} \bar{\mathbf{S}}_{ll} \right|, \tag{35}$$

where $\bar{\mathbf{S}}_{ll}$ and $\bar{\mathbf{\Psi}}_l^{\mathrm{d}}$ can be respectively expressed as follows

$$\bar{\mathbf{S}}_{ll} \triangleq N_{\mathrm{D}} \sqrt{\rho^{\mathrm{d}} \mu_l} \mathbf{\Gamma}_{ll}, \tag{36}$$

and

$$\bar{\mathbf{\Psi}}_l^{\mathrm{d}} = \rho^{\mathrm{d}} N_{\mathrm{D}}^2 \sum_{l' \neq l}^{L} \mu_{l'} \left(\beta_{l'l}^{\mathrm{d}} \Big/ \beta_{l'l'}^{\mathrm{d}}\right)^2 \mathrm{tr}\left(\left\|\mathbf{\Omega}_{ll'} \mathbf{\Gamma}_{l'l'}\right\|^2\right) \mathbf{I}_{N_{\mathrm{D}}}$$

$$R_l^{\mathrm{d}} = N_{\mathrm{D}} \log_2 \left(1 + \frac{\rho^{\mathrm{d}} N_{\mathrm{D}}^2 \mu_l \mathrm{tr}\left(\left\|\mathbf{\Gamma}_{ll}\right\|^2\right)}{\rho^{\mathrm{d}} N_{\mathrm{D}}^2 \sum\limits_{l' \neq l}^{L} \mu_{l'} \left(\beta_{l'l}^{\mathrm{d}} / \beta_{l'l'}^{\mathrm{d}}\right)^2 \mathrm{tr}\left(\left\|\mathbf{\Omega}_{ll'} \mathbf{\Gamma}_{l'l'}\right\|^2\right) + \Delta_l + \rho^{\mathrm{a}} N_{\mathrm{A}} \sum\limits_{m=1}^{M}\sum\limits_{j=1}^{J}\sum\limits_{k=1}^{K} \alpha_m \eta_{mjk} \beta_{ml}^{\mathrm{a}} + 1} \right), \tag{27}$$

$$\Delta_l = \rho^{\mathrm{d}} N_{\mathrm{D}} \sum_{l'=1}^{L} \mu_{l'} \beta_{l'l}^{\mathrm{d}} \left(\tau_{\mathrm{p}} \rho_{\mathrm{p}}^{\mathrm{d}} \beta_{l'l}^{\mathrm{d}} \mathrm{tr}\left(\left\|\mathbf{\Omega}_{ll'} \mathbf{C}_{l'l'}\right\|^2\right) + \left(\sum_{l'' \neq l}^{L} \beta_{l'l''}^{\mathrm{d}} + 1 \right) \mathrm{tr}\left(\left\|\mathbf{\Omega}_{l'} \mathbf{C}_{l'l'}\right\|^2\right) \right). \tag{28}$$

$$+\rho^{\mathrm{d}}N_{\mathrm{D}}\sum_{l'=1}^{L}\mu_{l'}\beta_{l'l}^{\mathrm{d}}\left(\tau_{\mathrm{p}}\rho_{\mathrm{p}}^{\mathrm{d}}\beta_{l'l}^{\mathrm{d}}\mathrm{tr}\left(\|\mathbf{\Omega}_{ll'}\mathbf{C}_{l'l'}\|^{2}\right)\right.$$
$$\left.+\left(\sum_{l''\neq l}^{L}\beta_{l'l''}^{\mathrm{d}}+1\right)\mathrm{tr}\left(\|\mathbf{\Omega}_{l'}\mathbf{C}_{l'l'}\|^{2}\right)\right)\mathbf{I}_{N_{\mathrm{D}}}$$
$$+\rho^{\mathrm{a}}N_{\mathrm{A}}\sum_{m=1}^{M}\sum_{j=1}^{J}\sum_{k=1}^{K}\alpha_{m}\eta_{mjk}\beta_{ml}^{\mathrm{a}}\mathbf{I}_{N_{\mathrm{D}}}+\mathbf{I}_{N_{\mathrm{D}}}. \quad (37)$$

Theorem 3: Using the random matrix theory, the lower bound on the achievable rate for the lth DUE receiver can be given as (27), shown at the bottom of the previous page.

Proof 3: Following a similar derivation as in the case of Theorem 2, Theorem 3 can be derived.

C. ASYMPTOTIC RATE ANALYSIS OF DUEs

Next, we then provide some insights into the achievable downlink rate of DUEs when M is very large, in this subsection. Based on the received signal for the kth CFUE in the jth group can be given by (29), we have

$$\mathbf{r}_{jk}^{\mathrm{c}}=\underbrace{\sqrt{\rho^{\mathrm{a}}}\sum_{m=1}^{M}\sum_{j=1}^{J}\sum_{k=1}^{K}\alpha_{m}\eta_{mjk}^{1/2}\left(\mathbf{G}_{mjk}^{\mathrm{a}}\right)^{H}\mathbf{Z}_{mj}^{\mathrm{a}}\mathbf{q}_{j}}_{\mathrm{DS}_{k}}$$
$$+\underbrace{\sqrt{\rho^{\mathrm{d}}}\sum_{l=1}^{L}\sqrt{u_{l}}\left(\mathbf{G}_{lk}^{\mathrm{d}}\right)^{H}\widehat{\mathbf{G}}_{ll}^{\mathrm{d}}\mathbf{s}_{l}}_{\mathrm{DUI}_{k}}$$
$$+\sum_{m=1}^{M}\left(\mathbf{G}_{mjk}^{\mathrm{a}}\right)^{H}\tilde{\mathbf{n}}_{m}+\mathbf{n}_{jk}, \quad (38)$$

where DS_k and DUI_k denote the desired signal and interference signal, respectively. By using the term $\mathbf{G}_{mjk}^{\mathrm{a}}=\widehat{\mathbf{G}}_{mjk}^{\mathrm{a}}+\mathbf{E}_{mjk}^{\mathrm{a}}$, we have

$$\left(\mathbf{G}_{mjk}^{\mathrm{a}}\right)^{H}\mathbf{Z}_{mj}^{\mathrm{a}}=\gamma_{mjk}^{1/2}\left(\mathbf{Z}_{mj}^{\mathrm{a}}\right)^{H}\mathbf{Z}_{mj}^{\mathrm{a}}=\gamma_{mjk}^{1/2}N\mathbf{I}_{N_{\mathrm{A}}}, \quad (39)$$

and

$$\left(\mathbf{G}_{lk}^{\mathrm{d}}\right)^{H}\widehat{\mathbf{G}}_{ll}^{\mathrm{d}}=\frac{\tau_{\mathrm{p}}\rho_{\mathrm{p}}^{\mathrm{d}}\beta_{lk}^{1/2}\beta_{ll}^{1/2}\sum_{l'=1}^{L}\beta_{ll'}^{\mathrm{d}}\mathbf{\Omega}_{l'l}}{\tau_{\mathrm{p}}\rho_{\mathrm{p}}^{\mathrm{d}}\sum_{l'=1}^{L}\beta_{ll'}^{\mathrm{d}}\mathbf{\Omega}_{l'l}^{H}\mathbf{\Omega}_{ll}+\mathbf{I}_{N_{\mathrm{D}}}}. \quad (40)$$

By using Tchebyshev's theorem as shown in [39], we have

$$\frac{1}{M}\mathrm{DS}_{k}-\frac{1}{M}\sqrt{\rho^{\mathrm{a}}}\sum_{m=1}^{M}\sum_{j=1}^{J}\sum_{k=1}^{K}\alpha_{m}\eta_{mjk}^{1/2}N\gamma_{mjk}^{1/2}\mathbf{I}_{N_{\mathrm{A}}}\mathbf{q}_{j}$$
$$\xrightarrow[M\to\infty]{a.s.}\mathbf{0}, \quad (41)$$

and

$$\frac{1}{M}\mathrm{DUI}_{k}-\frac{1}{M}\frac{\tau_{\mathrm{p}}\rho_{\mathrm{p}}^{\mathrm{d}}\beta_{lk}^{1/2}\beta_{ll}^{1/2}\sum_{l'=1}^{L}\beta_{ll'}^{\mathrm{d}}\mathbf{\Omega}_{l'l}}{\tau_{\mathrm{p}}\rho_{\mathrm{p}}^{\mathrm{d}}\sum_{l'=1}^{L}\beta_{ll'}^{\mathrm{d}}\mathbf{\Omega}_{l'l}^{H}\mathbf{\Omega}_{ll}+\mathbf{I}_{N_{\mathrm{D}}}}\xrightarrow[M\to\infty]{a.s.}\mathbf{0}. \quad (42)$$

Combining (41) and (42), therefore, the asymptotic analysis for the kth CFUE in the jth group can be given as follows (33), shown at the bottom of the page.

IV. ACHIEVABLE DOWNLINK SUM EE

In light of [21] and [32], the achievable downlink sum EE can be defined as follows

$$\eta_{\mathrm{EE}}\triangleq\frac{B\times R_{\mathrm{sum}}}{P_{\mathrm{sum}}}, \quad (43)$$

where the sum rate of the system under consideration can be given as

$$R_{\mathrm{sum}}=\sum_{j=1}^{J}\sum_{k=1}^{K}R_{jk}^{\mathrm{c}}+\sum_{l=1}^{L}R_{l}^{\mathrm{d}}, \quad (44)$$

where $L=D^{2}\lambda_{\mathrm{d}}$ denotes the average number of $\mathrm{DUE}_{l'}^{\mathrm{Rx}}$. Furthermore, R_{jk}^{c} and R_{l}^{d} are respectively given by (14) and (27). In addition, the λ_{d} denotes the DUEs' density obeying independent homogeneous Poisson point process (PPP). Furthermore, D^2 represents $D\times D$ coverage area where M APs, $J\times K$ CFUEs, and L DUE pairs are distributed as uniformly scattered.

The sum power consumption of the considered downlink D2D underlaid multigroup multicast cell-free massive MIMO systems with multi-antenna users can be modeled by

$$P_{\mathrm{sum}}=\sum_{m=1}^{M}P_{m}+\sum_{l=1}^{L}P_{l}+\sum_{m=1}^{M}\left(B\cdot R_{\mathrm{sum}}\cdot P_{\mathrm{bt},m}+P_{0,m}\right), \quad (45)$$

where B represents the system bandwidth, P_m, P_l, $P_{\mathrm{bt},m}$, and $P_{0,m}$ are the power costs at mth AP and lth $\mathrm{DUE}_{l}^{\mathrm{Rx}}$, the traffic-fronthaul power associated with the mth AP, and the fixed power consumption per fronthual link, respectively. To be more specific, the term P_m can be written as

$$P_{m}=N_{\mathrm{A}}\cdot P_{\mathrm{tc},m}+\frac{1}{\delta_{m}}\rho_{\mathrm{d}}^{\mathrm{a}}N_{0}\left(\alpha_{m}NN_{\mathrm{A}}\sum_{j=1}^{J}\left(\sum_{k=1}^{K}\eta_{mjk}^{1/2}\right)^{2}\right), \quad (46)$$

$$\frac{1}{M}\mathbf{r}_{jk}^{\mathrm{c}}-\frac{1}{M}\left(\sqrt{\rho^{\mathrm{a}}}\sum_{m=1}^{M}\sum_{j=1}^{J}\sum_{k=1}^{K}\alpha_{m}\eta_{mjk}^{1/2}N\gamma_{mjk}^{1/2}\mathbf{I}_{N_{\mathrm{A}}}\mathbf{q}_{j}+\frac{\tau_{\mathrm{p}}\rho_{\mathrm{p}}^{\mathrm{d}}\beta_{lk}^{1/2}\beta_{ll}^{1/2}\sum_{l'=1}^{L}\beta_{ll'}^{\mathrm{d}}\mathbf{\Omega}_{l'l}}{\tau_{\mathrm{p}}\rho_{\mathrm{p}}^{\mathrm{d}}\sum_{l'=1}^{L}\beta_{ll'}^{\mathrm{d}}\mathbf{\Omega}_{l'l}^{H}\mathbf{\Omega}_{ll}+\mathbf{I}_{N_{\mathrm{D}}}}\mathbf{s}_{l}\right)\xrightarrow[M\to\infty]{a.s.}\mathbf{0}. \quad (33)$$

where $0 \leq \delta_m \leq 1$ stand for the power amplifier efficiency, and the noise power. Besides, the power consumption at mth AP, $P_{\mathrm{tc},m}$, can be described as

$$P_{\mathrm{tc},m} = N_{\mathrm{A}}\left(c_{\mathrm{ADC},m}P_{\mathrm{AGC},m} + P_{\mathrm{ADC},m}\right) + N_{\mathrm{A}} \cdot P_{\mathrm{res},m} + N_{\mathrm{A}}\left(c_{\mathrm{ADC},m}P_{\mathrm{AGC},m} + P_{\mathrm{DAC},m}\right), \quad (47)$$

where $P_{\mathrm{AGC},m}$ and $P_{\mathrm{res},m}$ represent the power consumption of the automatic generation control (AGC) and the residual components at the mth AP. Additionally, the $P_{\mathrm{ADC},m}$ and $P_{\mathrm{DAC},m}$ can be denoted by

$$P_{\mathrm{ADC},m} = \frac{3V_{\mathrm{dd}}^2 L_{\min}\left(2B + f_{\mathrm{cor}}\right)}{10^{-0.1525b_m^{\mathrm{ADC}}+4.838}}, \quad (48)$$

and

$$P_{\mathrm{DAC},m} = \frac{1}{2}V_{\mathrm{dd}}I_0\left(2^{b_m^{\mathrm{DAC}}} - 1\right) + b_m^{\mathrm{DAC}}C_{\mathrm{p}}\left(2B + f_{\mathrm{cor}}\right)V_{\mathrm{dd}}^2, \quad (49)$$

where V_{dd}, C_{p}, f_{cor}, and I_0 remark the power supply of converter, the parasitic capacitance of each switch in converter, the corner frequency of the $1/f$, and the unit current source related to the least significant bit (LSB) is limited by the noise floor and device mismatch, respectively.

Moreover, the $c_{\mathrm{ADC},m}$ and $c_{\mathrm{DAC},m}$ indicate the sign associated with the low-resolution ADC/DAC precision $b_m^{\mathrm{ADC}}/b_m^{\mathrm{DAC}}$, which can be specified as

$$c_{\mathrm{ADC/DAC},m} = \begin{cases} 0, & b_m^{\mathrm{ADC}}/b_m^{\mathrm{DAC}} = 1 \\ 1, & b_m^{\mathrm{ADC}}/b_m^{\mathrm{DAC}} > 1. \end{cases} \quad (50)$$

Plugging the equations (46)-(50) into (45), and combining (43)-(44), the sum EE can be obtained after several simple algebraic calculations.

V. SIMULATION RESULTS

In this section, the performance analysis of the derived results is evaluated to verify our analytical result and evaluate the performance of D2D underlaid multigroup multicast cell-free massive MIMO for multi-antenna at both the APs and users, as well as other key parameters.

A. PARAMETERS SETUPS

In this paper, we primarily focus on the scenario with $JK = 10$ CFUEs, $N_{\mathrm{D}} = 2$ antennas of DUEs. All APs and CFUEs are uniformly and randomly scattered in the square area of 1 [km^2]. For the sake of analysis, we assume $\lambda_m = \alpha_m = 5, \forall m$. This area is also wrapped around to avoid the boundary effects as well. We only consider the effect of low-resolution DACs due to the fact that the uplink estimation is very similar to the downlink transmission. Besides, the DUEs are represented as an independent homogeneous PPP with the density λ_{d} and the three-slope path loss model is adopted. Unless specifically mentioned, the other parameters setups are given as in [7], [21], and [32].

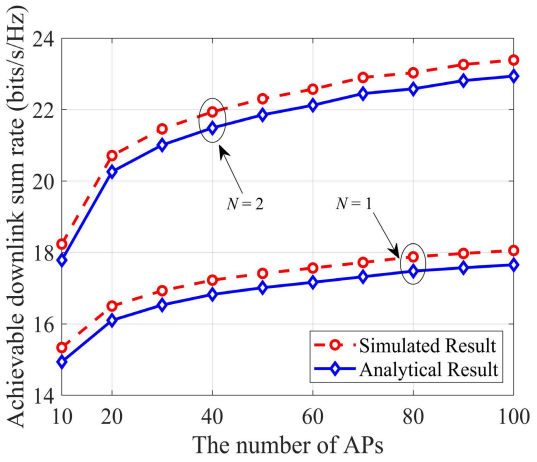

FIGURE 2. Achievable downlink sum rate versus the number of APs for different K, with $L = 10$, $N_{\mathrm{D}} = 2$.

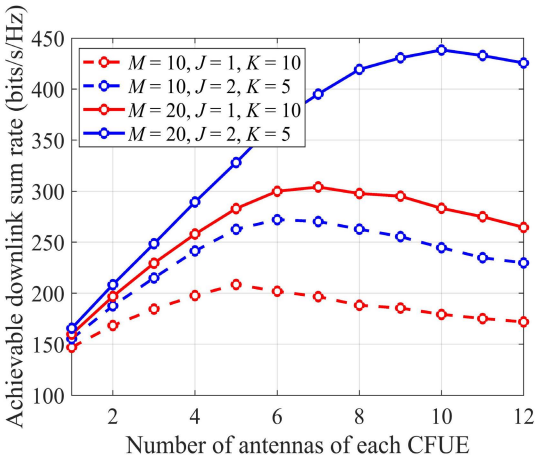

FIGURE 3. Achievable downlink sum rate versus the number of antennas of each CFUEs, with $N_{\mathrm{A}} = 5$, $N = 2$.

B. PERFORMANCE EVALUATION

First, the achievable downlink sum rate versus the number of APs for different K are exhibited in Fig. 2, with $L = 10, N_{\mathrm{D}} = 2$. Note that, all Simulated Results are based on (30), (35) and obtained by averaging over 10^4 independent channel realizations, while the Analytical Results are generated according to (14), (27). As can be readily observed, due to the interference and estimation error, the relative performance gaps of the achievable sum rate are marginal, confirming the accuracy of our analytical finding.

Next, we depict the achievable downlink sum rate versus the number of antennas of each CFUE in Fig. 3, where $N_{\mathrm{A}} = 5, N = 2$. From the results we can know that the achievable sum rate for the multicast multigroup configuration $J = 2, K = 5$ precedes the one of the unicast $J = 1, K = 10$. The results show that the achievable sum rate behaves differently in scenarios with a low and high number of antennas of CFUEs. To be more specific, when the antennas of each CFUE are lower than the optimal value, the achievable sum rate increases with it consensually grows and vice versa. This fully demonstrates the significant benefits of the multigroup

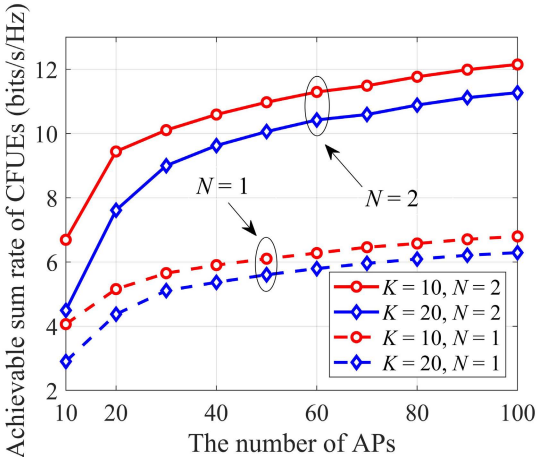

FIGURE 4. Achievable sum rate of CFUEs versus the number of APs, with $L = 10, N_D = 2$.

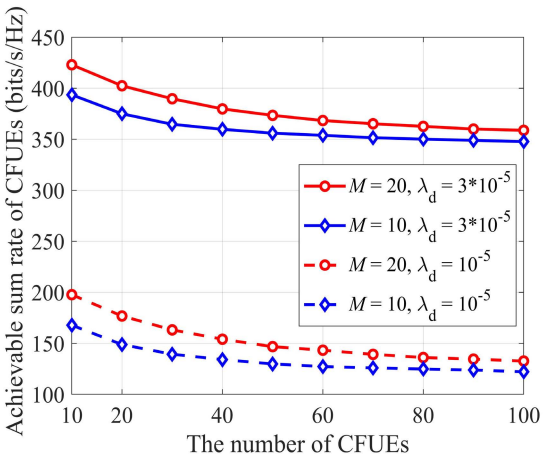

FIGURE 6. Achievable downlink CFUEs rate versus the number of CFUEs, with $L = 10, N = 2$.

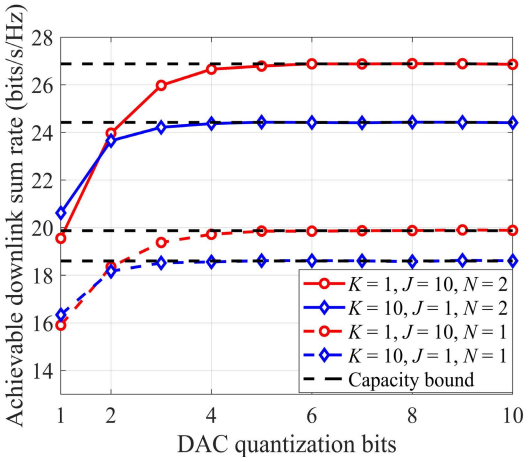

FIGURE 5. Achievable downlink sum rate versus the DAC quantization bits, with $N_A = 20, N_D = 2$.

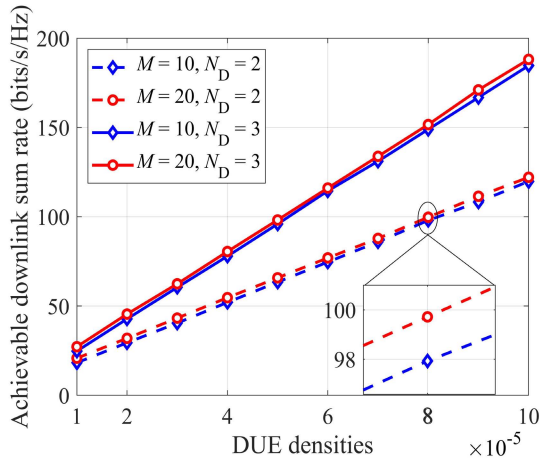

FIGURE 7. Achievable downlink sum rate versus the DUE densities, with $N_A = 20, JK = 10$.

multicast strategy in D2D underlaid cell-free massive MIMO systems.

In Fig. 4, the achievable sum rate of CFUEs versus the number of APs is given, where $L = 10, N_D = 2$. It shows that the sum rate of CFUEs increases with the number of APs. The reason for this is that having a large numbers of APs allows for more favorable channels and excellent channel hardening performance. Despite this, the greater the number of the AP antennas, the greater the multiplexing gain and spatial freedom for the system.

Fig. 5 describes the achievable downlink sum rate against the DAC quantization bits, with $N_A = 20, N_D = 2$. As the obtained results despited in Fig. 2, the achievable sum rate for the multicast multigroup precedes the one of the unicast both for the antennas of APs of $N = 2$ and $N = 1$. Besides, we also can obtain that with the DAC quantization bits increases, the achievable sum rate can be improved with the fact that the corresponding quantization noise decrease when $b_m^{\mathrm{DAC}} \leq 5$; while as further increases, the sum rate for different configurations all grows slowly and eventually converges to each capacity limit.

In Fig. 6, the achievable downlink rate of CFUEs versus the number of CFUEs is presented, with $L = 10, N = 2$. For the current simulation setup, we can see that the rate of CFUEs decreases as the number of the CFUEs increases. The reason for this is that large amounts of DUEs and CUEs will cause serious interference such as pilot contamination, CFUEs-DUEs, DUEs-DUEs, and CFUEs-DUEs, thus deteriorating the performance of the considered system.

In Fig. 7, the achievable downlink sum rate against the DUE densities is plotted, with $N_A = 20, JK = 10$. With the derived results we can deduce from the sum rate increases nearly linearly with the density of DUEs. It fully illustrates the enormous benefits of D2D communication underlaid to improve the sum SE of the system. To be more specific, using multiple antennas at DUEs can also sharply boost the system performance.

In Fig. 8, the achievable downlink sum rate versus the number of antennas at each AP, with $N = 2, N_D = 2$, is provided. We see that increasing the number of antennas of each AP can effectively improve the achievable the sum rate. The reason is that the more APs deployed, the more favorable

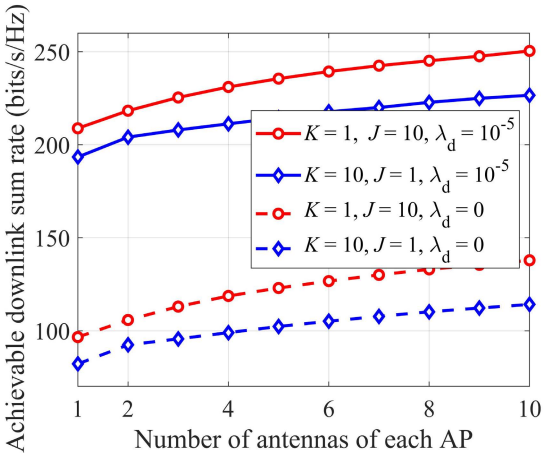

FIGURE 8. Achievable downlink sum rate versus the number of antennas at each AP, with $N = 2$, $N_D = 2$.

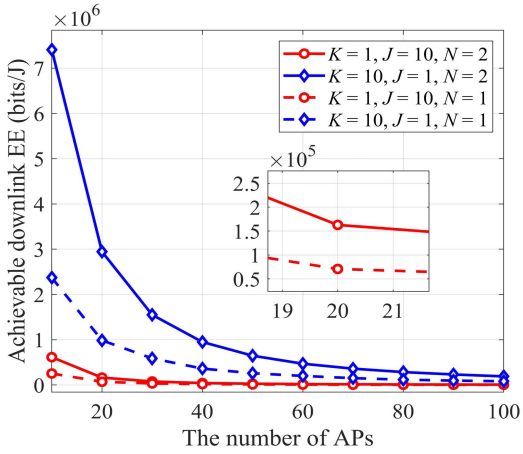

FIGURE 9. Achievable downlink sum EE versus the number of APs, with $L = 10, N_D = 2$.

of the transmission channel and thus the more obvious the channel hardening. To be specific, the diversity gain and multiplexing gain can be obtained by the light of nature. Furthermore, as despited in Figs. 6 and 7, the achievable sum rate can be improved by increasing the density of DUEs.

Up till now, the achievable sum rate for the considered D2D underlaid multigroup multicast cell-free massive MIMO with multi-antenna users has been explored. Next, the performance of sum EE is then exhibited. In Fig. 9, the effects of the achievable sum EE against the number of the APs are shown first, with $L = 10, N_D = 2$. The simulation results show that the sum EE decreases with the number of the APs sharply due to the fact that sum rate gains by employing much APs are less than the sum energy consumption by the introduced APs.

In Fig. 10, the network performance in terms of the sum EE against the DAC quantization bits is given, with $M = 20, N_A = 10$. We can observe that the indeed the low DAC bits scenario does benefits in terms of the consumption by the DAC dominates the performance and rapidly leads to a gradual decrease in sum EE. As the figure implies, there exists an optimal number of DAC quantization bits, $b_m^{DAC} = 2$, for the maximum sum EE.

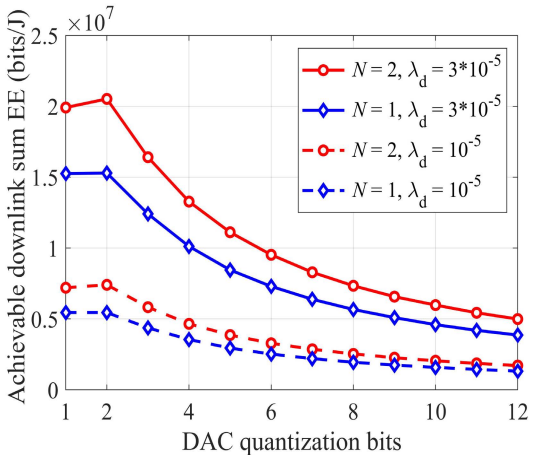

FIGURE 10. Achievable downlink sum EE versus the DAC quantization bits, with $M = 20, N_A = 10$.

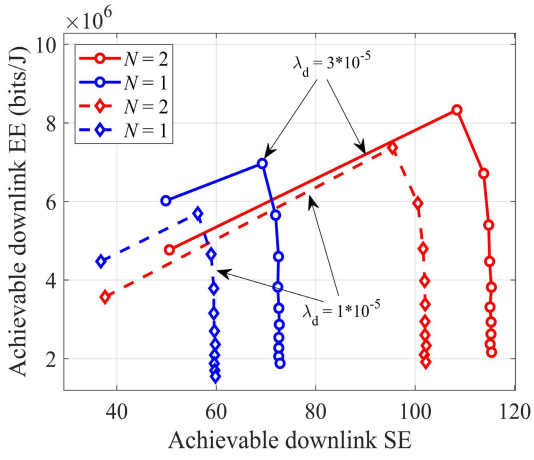

FIGURE 11. The tradeoff between the sum EE and sum SE versus the DAC quantization bits, with $M = 20, N_A = 10$.

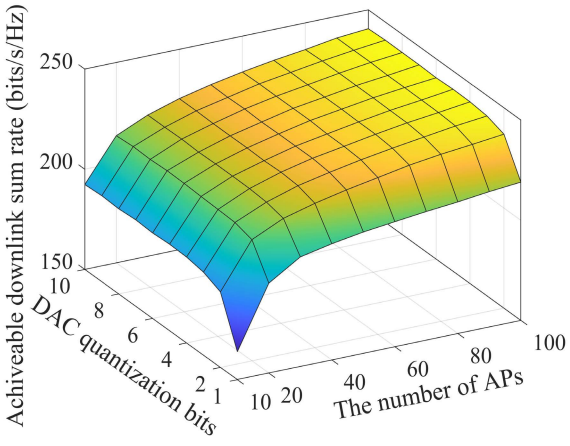

FIGURE 12. Joint impact of the number of APs and DAC quantization bits on sum rate, with $N = 2, N_D = 2$.

In Fig. 11, the tradeoff between the sum EE and sum SE versus the DAC quantization bits is expressed, with $M = 20, N_A = 10$. It should be noticed that the resultant curves are plotted by letting the value of bits vary from 1 to 11 with steps

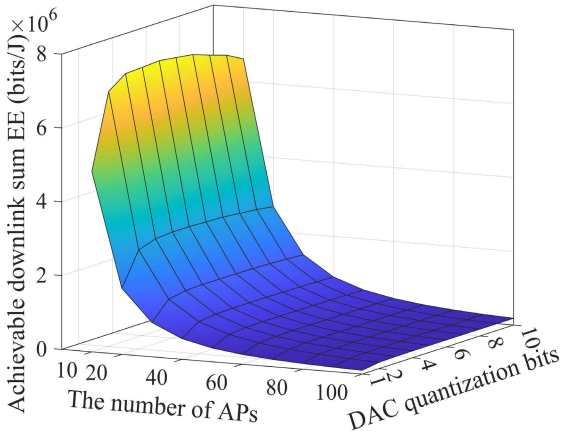

FIGURE 13. Joint impact of the number of APs and DAC quantization bits on sum EE, with $L = 10, N_D = 2$.

of 1. We can see that the rightmost point indicates the largest sum rate value while the highest point means the largest sum EE value. As a supplement, Figs. 12 and 13 give the joint impact of the number of APs and DAC quantization bits on both the achievable sum rate and sum EE.

VI. CONCLUSION

In this paper, the downlink D2D underlaid multigroup multicast cell-free massive MIMO systems with multi-antenna users have been considered, where the DUEs are distributed according to PPP. Assuming that the imperfect CSI can be acquired, the achievable rates of both CFUEs and DUEs are calculated. Following that, the sum EE is conducted using the constructed energy consumption model. The obtained results allow us to quantitatively investigate the effects of the number/antenna of APs/CFUEs/DUEs, the density of DUEs, and the quantization bits. To be more specific, increasing the number of APs can improve the sum SE, however, the sum EE decreases with the number of the APs sharply. The obtained results demonstrate the significance of the collaborative deployment of D2D and multigroup multicast cell-free massive MIMO technology, providing important references and guidance for future practical deployments of B5G/6G.

APPENDICES

A. PROOF OF THEOREM 1

For the sake of analysis, we first calculate the following values:

$$\begin{aligned}
&\mathbb{E}\left\{\widetilde{\mathbf{W}}_{\mathrm{p},m}^{H}\widetilde{\mathbf{W}}_{\mathrm{p},m}\right\}\\
&=\lambda_m\left(1-\lambda_m\right)\mathrm{diag}\left(\mathbb{E}\left\{\mathbf{Y}_{\mathrm{p},mj}^{\mathrm{a}}\left(\mathbf{Y}_{\mathrm{p},mj}^{\mathrm{a}}\right)^{H}\right\}\right)\\
&=N_{\mathrm{A}}\lambda_m\left(1-\lambda_m\right)\left(\tau_{\mathrm{p}}\rho_{\mathrm{p}}^{\mathrm{c}}\sum_{j'=1}^{J}\sum_{k'=1}^{K}\beta_{mj'k'}\left\|\boldsymbol{\Phi}_{j'}^{H}\boldsymbol{\Phi}_{j}\right\|^{2}+\mathbf{I}_{\tau_{\mathrm{p}}}\right).
\end{aligned}\tag{51}$$

By using (6), we have

$$\begin{aligned}
&\mathbb{E}\left\{\left(\mathbf{G}_{mjk}^{\mathrm{a}}\right)^{H}\widetilde{\mathbf{Y}}_{\mathrm{p},mj}^{\mathrm{a}}\right\}\\
&=\mathbb{E}\left\{\lambda_m\sqrt{\tau_{\mathrm{p}}\rho_{\mathrm{p}}^{\mathrm{c}}}\sum_{j=1}^{J}\sum_{k=1}^{K}\left(\mathbf{G}_{mjk}^{\mathrm{a}}\right)^{H}\mathbf{G}_{mjk}^{\mathrm{a}}\right\}\\
&\quad+\mathbb{E}\left\{\lambda_m\left(\mathbf{G}_{mjk}^{\mathrm{a}}\right)^{H}\widetilde{\mathbf{W}}_{\mathrm{p},mj}\right\}+\mathbb{E}\left\{\left(\mathbf{G}_{mjk}^{\mathrm{a}}\right)^{H}\widetilde{\mathbf{W}}_{\mathrm{p},m}\right\}\\
&=N_{\mathrm{A}}\lambda_m\sqrt{\tau_{\mathrm{p}}\rho_{\mathrm{p}}^{\mathrm{c}}}\beta_{mjk}.
\end{aligned}\tag{52}$$

Therefore, the $\mathbb{E}\left\{\left\|\widetilde{\mathbf{Y}}_{\mathrm{p},mj}^{\mathrm{a}}\right\|^{2}\right\}$ can be derived as

$$\begin{aligned}
&\mathbb{E}\left\{\left\|\widetilde{\mathbf{Y}}_{\mathrm{p},mj}^{\mathrm{a}}\right\|^{2}\right\}\\
&=N_{\mathrm{A}}\lambda_m^{2}\tau_{\mathrm{p}}\rho_{\mathrm{p}}^{\mathrm{c}}\sum_{j'=1}^{J}\sum_{k'=1}^{K}\beta_{mjk'}\left\|\boldsymbol{\Phi}_{j'}^{H}\boldsymbol{\Phi}_{j}\right\|^{2}+N_{\mathrm{A}}\lambda_m^{2}\mathbf{I}_N\\
&\quad+N_{\mathrm{A}}\lambda_m\left(1-\lambda_m\right)\left(\tau_{\mathrm{p}}\rho_{\mathrm{p}}^{\mathrm{c}}\sum_{j'=1}^{J}\sum_{k'=1}^{K}\beta_{mjk'}\left\|\boldsymbol{\Phi}_{j'}^{H}\boldsymbol{\Phi}_{j}\right\|^{2}+\mathbf{I}_N\right)\\
&=N_{\mathrm{A}}\lambda_m\tau_{\mathrm{p}}\rho_{\mathrm{p}}^{\mathrm{c}}\left(\sum_{j'=1}^{J}\sum_{k'=1}^{K}\beta_{mjk'}\left\|\boldsymbol{\Phi}_{j'}^{H}\boldsymbol{\Phi}_{j}\right\|^{2}+\mathbf{I}_N\right).
\end{aligned}\tag{53}$$

To that end, the estimated channel $\widehat{\mathbf{G}}_{mjk}^{\mathrm{a}}$ can be derived as

$$\begin{aligned}
\widehat{\mathbf{G}}_{mjk}^{\mathrm{a}}&=\frac{\mathbb{E}\left\{\mathbf{G}_{mjk}^{\mathrm{a}}\left(\widetilde{\mathbf{Y}}_{\mathrm{p},mj}^{\mathrm{a}}\right)^{H}\right\}}{\mathbb{E}\left\{\left\|\widetilde{\mathbf{Y}}_{\mathrm{p},mj}^{\mathrm{a}}\right\|^{2}\right\}}\widetilde{\mathbf{Y}}_{\mathrm{p},mj}^{\mathrm{a}}\\
&=\frac{\sqrt{\tau_{\mathrm{p}}\rho_{\mathrm{p}}^{\mathrm{c}}}\beta_{mjk}}{\tau_{\mathrm{p}}\rho_{\mathrm{p}}^{\mathrm{c}}\sum_{j'=1}^{J}\sum_{k'=1}^{K}\beta_{mjk'}\left\|\boldsymbol{\Phi}_{j'}^{H}\boldsymbol{\Phi}_{j}\right\|^{2}+\mathbf{I}_N}\widetilde{\mathbf{Y}}_{\mathrm{p},mj}^{\mathrm{a}}.
\end{aligned}\tag{54}$$

Combining (6) and (54), we have

$$\left(\widehat{\mathbf{G}}_{mjk}^{\mathrm{a}}\right)^{H}\widehat{\mathbf{G}}_{mjk}^{\mathrm{a}}=N_{\mathrm{A}}\frac{\lambda_m\sqrt{\tau_{\mathrm{p}}\rho_{\mathrm{p}}^{\mathrm{c}}}\beta_{mjk}}{\tau_{\mathrm{p}}\rho_{\mathrm{p}}^{\mathrm{c}}\sum_{j'=1}^{J}\sum_{k'=1}^{K}\beta_{mjk'}\left\|\boldsymbol{\Phi}_{j'}^{H}\boldsymbol{\Phi}_{j}\right\|^{2}+\mathbf{I}_N}.\tag{55}$$

Based on the previous consideration, we can complete the proof of Theorem 1 by skipping the tedious derivation.

B. PROOF OF THEOREM 2

From (31) we can know that

$$\begin{aligned}
\bar{\mathbf{H}}_{jk}&=\mathbb{E}\left\{\sqrt{\rho_{\mathrm{d}}^{\mathrm{a}}}\sum_{m=1}^{M}\sum_{k'=1}^{K}\alpha_m\eta_{mjk'}^{1/2}\mathbf{G}_{mjk}^{\mathrm{a}}\mathbf{Z}_{mj}^{\mathrm{a}}\right\}\\
&=\mathbb{E}\left\{\sqrt{\rho_{\mathrm{d}}^{\mathrm{a}}}\sum_{m=1}^{M}\sum_{k'=1}^{K}\alpha_m\eta_{mjk'}^{1/2}\left(\widehat{\mathbf{G}}_{mjk}^{\mathrm{a}}+\mathbf{E}_{mjk}^{\mathrm{a}}\right)\mathbf{Z}_{mj}^{\mathrm{a}}\right\},
\end{aligned}\tag{56}$$

where $\mathbf{G}_{mjk}^{\mathrm{a}}=\widehat{\mathbf{G}}_{mjk}^{\mathrm{a}}+\mathbf{E}_{mjk}^{\mathrm{a}}$.

With the above consideration, $\bar{\mathbf{H}}_{jk}^H\bar{\mathbf{H}}_{jk}$ can be, mathematically, given as

$$\begin{aligned}
&\bar{\mathbf{H}}_{jk}^H\bar{\mathbf{H}}_{jk}\\
&= \mathbb{E}\left\{\sqrt{\rho_{\mathrm{d}}^{\mathrm{a}}}\sum_{m=1}^{M}\sum_{k'=1}^{K}\alpha_m\eta_{mjk'}^{1/2}\left(\left(\widehat{\mathbf{G}}_{mjk}^{\mathrm{a}}+\mathbf{E}_{mjk}^{\mathrm{a}}\right)\mathbf{Z}_{mj}^{\mathrm{a}}\right)^H\right\}\\
&\quad\times\mathbb{E}\left\{\sqrt{\rho_{\mathrm{d}}^{\mathrm{a}}}\sum_{m=1}^{M}\sum_{k'=1}^{K}\alpha_m\eta_{mjk'}^{1/2}\left(\widehat{\mathbf{G}}_{mjk}^{\mathrm{a}}+\mathbf{E}_{mjk}^{\mathrm{a}}\right)\mathbf{Z}_{mj}^{\mathrm{a}}\right\}\\
&= \left(N_{\mathrm{A}}\sqrt{\rho_{\mathrm{d}}^{\mathrm{a}}}\sum_{m=1}^{M}\sum_{k'=1}^{K}\alpha_m\eta_{mjk'}^{1/2}\gamma_{mjk}^{1/2}\right)^2\mathbf{I}_N. \qquad (57)
\end{aligned}$$

By virtue of the (29) and (31), we have the following calculations

$$\begin{aligned}
\boldsymbol{\Psi}_{jk}^{\mathrm{c}} &= \mathbb{E}\left\{\mathbf{r}_{jk}^{\mathrm{c}}\left(\mathbf{r}_{jk}^{\mathrm{c}}\right)^H|\bar{\mathbf{H}}_{jk}\right\}\\
&= \mathbb{E}\left\{\rho_{\mathrm{d}}^{\mathrm{a}}\sum_{m=1}^{M}\sum_{n=1}^{N}\sum_{j'=1}^{J}\sum_{k'=1}^{K}\sum_{k''=1}^{K}\alpha_m\alpha_n\eta_{mj'k'}^{1/2}\eta_{njk''}^{1/2}\left(\mathbf{G}_{mjk}^{\mathrm{a}}\right)^H\right.\\
&\quad\times\mathbf{Z}_{mj'}^{\mathrm{a}}\left(\mathbf{Z}_{nj'}^{\mathrm{a}}\right)^H\mathbf{G}_{njk}^{\mathrm{a}}+\sum_{m=1}^{M}\left(\mathbf{G}_{mjk}^{\mathrm{a}}\right)^H\tilde{\mathbf{n}}_m\tilde{\mathbf{n}}_m^H\mathbf{G}_{mjk}^{\mathrm{a}}\\
&\quad\left.+\sum_{l=1}^{L}\rho^{\mathrm{d}}\mu_l\left(\mathbf{G}_{lk}^{\mathrm{d}}\right)^H\widehat{\mathbf{G}}_{ll}^{\mathrm{d}}\left(\widehat{\mathbf{G}}_{ll}^{\mathrm{d}}\right)^H\mathbf{G}_{lk}^{\mathrm{d}}+\mathbf{I}_N\right\}. \qquad (58)
\end{aligned}$$

With the fact that $\bar{\boldsymbol{\Psi}}_{jk}^{\mathrm{c}}=\boldsymbol{\Psi}_{jk}^{\mathrm{c}}-\bar{\mathbf{H}}_{jk}^H\bar{\mathbf{H}}_{jk}$, we can complete the proof of the Theorem 2 after several algebraic calculations by combining the equations of (56)-(58).

C. PROOF OF THEOREM 3

With the equation (36), we have

$$\bar{\mathbf{S}}_{ll}^H\bar{\mathbf{S}}_{ll}=\rho^{\mathrm{d}}N_{\mathrm{D}}^2\sum_{l'=l}^{L}\mu_{l'}\left(\boldsymbol{\Omega}_{ll'}\boldsymbol{\Gamma}_{l'l}\boldsymbol{\Gamma}_{l'l}^H\boldsymbol{\Omega}_{ll'}^H\right). \qquad (59)$$

By using (34) and (36), then

$$\begin{aligned}
\boldsymbol{\Psi}_l^{\mathrm{d}} &= \mathbb{E}\left\{\mathbf{r}_l^{\mathrm{d}}\left(\mathbf{r}_l^{\mathrm{d}}\right)^H|\bar{\mathbf{S}}_{ll}\right\}\\
&= \mathbb{E}\left\{\mathbf{S}_{l'l'}\mathbf{S}_{l'l'}^H\right\}+\mathbb{E}\left\{\mathbf{n}_l\mathbf{n}_l^H\right\}\\
&\quad+\mathbb{E}\left\{\sum_{m=1}^{M}\left(\mathbf{G}_{ml}^{\mathrm{a}}\right)^H\tilde{\mathbf{n}}_m\tilde{\mathbf{n}}_m^H\mathbf{G}_{ml}^{\mathrm{a}}\right\}\\
&\quad+\mathbb{E}\left\{\sum_{m=1}^{M}\sum_{j=1}^{J}\sum_{k=1}^{K}\alpha_m^2\left(\mathbf{G}_{ml}^{\mathrm{a}}\right)^H\mathbf{Z}_{mj}^{\mathrm{a}}\left(\mathbf{Z}_{mj}^{\mathrm{a}}\right)^H\mathbf{G}_{ml}^{\mathrm{a}}\right\}. \qquad (60)
\end{aligned}$$

The term $\mathbb{E}\left\{\mathbf{S}_{l'l'}\mathbf{S}_{l'l'}^H\right\}$ in $\boldsymbol{\Psi}_l^{\mathrm{d}}$ can be first calculated as

$$\begin{aligned}
\mathbb{E}\left\{\mathbf{S}_{l'l'}\mathbf{S}_{l'l'}^H\right\} &= \mathbb{E}\left\{\rho^{\mathrm{d}}\sum_{l'=1}^{L}\mu_{l'}\left(\mathbf{G}_{l'l}^{\mathrm{d}}\right)^H\widehat{\mathbf{G}}_{l'l'}^{\mathrm{d}}\left(\widehat{\mathbf{G}}_{l'l'}^{\mathrm{d}}\right)^H\mathbf{G}_{l'l}^{\mathrm{d}}\right\}\\
&= \rho^{\mathrm{d}}\left(\tau_{\mathrm{p}}\rho_{\mathrm{p}}^{\mathrm{d}}\sum_{l'=1}^{L}\mathbf{D}_{11}+\tau_{\mathrm{p}}\rho_{\mathrm{p}}^{\mathrm{d}}\sum_{l''\neq l}^{L}\mathbf{D}_{12}+\mathbf{D}_{13}\right), \qquad (61)
\end{aligned}$$

where $\mathbf{D}_{11}$, $\mathbf{D}_{12}$, and $\mathbf{D}_{13}$ can be derived as, respectively

$$\begin{aligned}
\mathbf{D}_{11} &= \mathbb{E}\left\{\left(\mathbf{G}_{l'l}^{\mathrm{d}}\right)^H\mathbf{G}_{l'l}^{\mathrm{d}}\underbrace{\boldsymbol{\Omega}_{ll'}\mathbf{C}_{l'l'}\mathbf{C}_{l'l'}^H\boldsymbol{\Omega}_{ll'}^H}_{\mathbf{B}_{l'l}}\left(\mathbf{G}_{l'l}^{\mathrm{d}}\right)^H\mathbf{G}_{l'l}^{\mathrm{d}}\right\}\\
&\overset{(a)}{=} N_{\mathrm{D}}\left(\beta_{l'l}^{\mathrm{d}}\right)^2\mathbf{J}_{ll'}\\
&= N_{\mathrm{D}}\left(\beta_{l'l}^{\mathrm{d}}\right)^2\mathrm{tr}\left(\boldsymbol{\Omega}_{ll'}\mathbf{C}_{l'l'}\mathbf{C}_{l'l'}^H\boldsymbol{\Omega}_{ll'}^H\right)\mathbf{I}_{N_{\mathrm{D}}}\\
&\quad+N_{\mathrm{D}}^2\left(\beta_{l'l}^{\mathrm{d}}\Big/\sqrt{\tau_{\mathrm{p}}\rho_{\mathrm{p}}^{\mathrm{d}}}\beta_{l'l'}^{\mathrm{d}}\right)^2\left(\boldsymbol{\Omega}_{ll'}\mathbf{C}_{l'l'}\mathbf{C}_{l'l'}^H\boldsymbol{\Omega}_{ll'}^H\right), \qquad (62)
\end{aligned}$$

and

$$\begin{aligned}
\mathbf{D}_{12} &= \mathbb{E}\left\{\left(\mathbf{G}_{l'l}^{\mathrm{d}}\right)^H\mathbf{G}_{l'l''}^{\mathrm{d}}\boldsymbol{\Omega}_{l'}\mathbf{C}_{l'l'}\mathbf{C}_{l'l'}^H\boldsymbol{\Omega}_{l'}^H\left(\mathbf{G}_{l'l''}^{\mathrm{d}}\right)^H\mathbf{G}_{l'l}^{\mathrm{d}}\right\}\\
&= N_{\mathrm{D}}\beta_{l'l}^{\mathrm{d}}\beta_{l'l''}^{\mathrm{d}}\mathrm{tr}\left(\boldsymbol{\Omega}_{l'}\mathbf{C}_{l'l'}\mathbf{C}_{l'l'}^H\boldsymbol{\Omega}_{l'}^H\right)\mathbf{I}_{N_{\mathrm{D}}}, \qquad (63)
\end{aligned}$$

and

$$\begin{aligned}
\mathbf{D}_{13} &= \mathbb{E}\left\{\left(\mathbf{G}_{l'l}^{\mathrm{d}}\right)^H\mathbf{W}_{\mathrm{p},l}^{\mathrm{d}}\boldsymbol{\Omega}_{l'}\mathbf{C}_{l'l'}\mathbf{C}_{l'l'}^H\boldsymbol{\Omega}_{l'}^H\mathbf{W}_{\mathrm{p},l}^{\mathrm{d}}\mathbf{G}_{l'l}^{\mathrm{d}}\right\}\\
&= N_{\mathrm{D}}\beta_{l'l}^{\mathrm{d}}\mathrm{tr}\left(\boldsymbol{\Omega}_{l'}\mathbf{C}_{l'l'}\mathbf{C}_{l'l'}^H\boldsymbol{\Omega}_{l'}^H\right)\mathbf{I}_{N_{\mathrm{D}}}, \qquad (64)
\end{aligned}$$

where (a) is given by $\mathbf{J}_{ll'}$ as

$$\mathbf{J}_{ll'}=\mathrm{tr}\left(\mathbf{B}_{l'l}\right)\mathbf{I}_{N_{\mathrm{D}}}+N_{\mathrm{D}}\mathrm{diag}\left(\mathbf{B}_{l'l}\right), \qquad (65)$$

and the element of $\mathbf{J}_{ll'}$ is given as follows

$$j_{ll}=\sum_{l}^{L}b_{ll}+N_{\mathrm{D}}b_{ll}. \qquad (66)$$

The substitution of (62), (63), and (64) into (61), then the $\mathbb{E}\left\{\mathbf{S}_{l'l'}\mathbf{S}_{l'l'}^H\right\}$ can be given further as

$$\begin{aligned}
&\mathbb{E}\left\{\mathbf{S}_{l'l'}\mathbf{S}_{l'l'}^H\right\}\\
&= \rho^{\mathrm{d}}N_{\mathrm{D}}\sum_{l'=1}^{L}\mu_{l'}\left(\tau_{\mathrm{p}}\rho_{\mathrm{p}}^{\mathrm{d}}\left(\beta_{l'l}^{\mathrm{d}}\right)^2\mathrm{tr}\left(\boldsymbol{\Omega}_{ll'}\mathbf{C}_{l'l'}\mathbf{C}_{l'l'}^H\boldsymbol{\Omega}_{ll'}^H\right)\mathbf{I}_{N_{\mathrm{D}}}\right.\\
&\quad+N_{\mathrm{D}}\left(\beta_{l'l}^{\mathrm{d}}\Big/\beta_{l'l'}^{\mathrm{d}}\right)^2\left.\left(\boldsymbol{\Omega}_{ll'}\boldsymbol{\Gamma}_{l'l'}\boldsymbol{\Gamma}_{l'l'}^H\boldsymbol{\Omega}_{ll'}^H\right)\right)\\
&\quad+\rho^{\mathrm{d}}N_{\mathrm{D}}\sum_{l'=1}^{L}\sum_{l''\neq l}^{L}\mu_{l'}\beta_{l'l}^{\mathrm{d}}\beta_{l'l''}^{\mathrm{d}}\mathrm{tr}\left(\boldsymbol{\Omega}_{l'}\mathbf{C}_{l'l'}\mathbf{C}_{l'l'}^H\boldsymbol{\Omega}_{l'}^H\right)\mathbf{I}_{N_{\mathrm{D}}}\\
&\quad+\rho^{\mathrm{d}}N_{\mathrm{D}}\sum_{l'=1}^{L}\mu_{l'}\beta_{l'l}^{\mathrm{d}}\mathrm{tr}\left(\boldsymbol{\Omega}_{l'}\mathbf{C}_{l'l'}\mathbf{C}_{l'l'}^H\boldsymbol{\Omega}_{l'}^H\right)\mathbf{I}_{N_{\mathrm{D}}}. \qquad (67)
\end{aligned}$$

To be more specific, we can calculate the following

$$\bar{\boldsymbol{\Psi}}_l^{\mathrm{d}}=\boldsymbol{\Psi}_l^{\mathrm{d}}-\bar{\mathbf{S}}_{ll}\bar{\mathbf{S}}_{ll}^H$$

$$= \rho^{\mathrm{d}} N_{\mathrm{D}}^2 \sum_{l' \neq l}^{L} \mu_{l'} \left(\beta_{l'l}^{\mathrm{d}} \Big/ \beta_{l'l'}^{\mathrm{d}} \right)^2 \mathrm{tr}\left(\|\mathbf{\Omega}_{ll'} \mathbf{\Gamma}_{l'l'}\|^2 \right) \mathbf{I}_{N_{\mathrm{D}}}$$
$$+ \rho^{\mathrm{d}} N_{\mathrm{D}} \sum_{l'=1}^{L} \mu_{l'} \beta_{l'l}^{\mathrm{d}} \left(\tau_{\mathrm{p}} \rho_{\mathrm{p}}^{\mathrm{d}} \beta_{l'l}^{\mathrm{d}} \mathrm{tr}\left(\|\mathbf{\Omega}_{ll'} \mathbf{C}_{l'l'}\|^2 \right) \right.$$
$$\left. + \left(\sum_{l'' \neq l}^{L} \beta_{l'l''}^{\mathrm{d}} + 1 \right) \mathrm{tr}\left(\|\mathbf{\Omega}_{l'} \mathbf{C}_{l'l'}\|^2 \right) \right) \mathbf{I}_{N_{\mathrm{D}}}$$
$$+ \rho^{\mathrm{a}} N N_{\mathrm{A}} \sum_{m=1}^{M} \sum_{j=1}^{J} \alpha_m \left(1 - \alpha_m\right) \beta_{ml}^{\mathrm{a}} \left(\sum_{k=1}^{K} \eta_{mjk}^{1/2} \right)^2$$
$$+ \rho^{\mathrm{a}} N N_{\mathrm{A}} \sum_{m=1}^{M} \sum_{j=1}^{J} \sum_{k=1}^{K} \alpha_m^2 \eta_{mjk} \beta_{ml}^{\mathrm{a}} \mathbf{I}_{N_{\mathrm{D}}} + \mathbf{I}_{N_{\mathrm{D}}}. \quad (68)$$

Combining the (61) and (67), the proof of Theorem 3 can be completed after several algebraic derivations.

REFERENCES

[1] H. Q. Ngo, A. Ashikhmin, H. Yang, E. G. Larsson, and T. L. Marzetta, "Cell-free massive MIMO: Uniformly great service for everyone," in *Proc. IEEE 16th Int. Workshop Signal Process. Adv. Wireless Commun. (SPAWC)*, Aug. 2015, pp. 201–205.

[2] H. Q. Ngo, A. Ashikhmin, H. Yang, E. G. Larsson, and T. L. Marzetta, "Cell-free massive MIMO versus small cells," *IEEE Trans. Wireless Commun.*, vol. 16, no. 3, pp. 1834–1850, Mar. 2017.

[3] H. A. Ammar, R. Adve, S. Shahbazpanahi, G. Boudreau, and K. V. Srinivas, "User-centric cell-free massive MIMO networks: A survey of opportunities, challenges and solutions," *IEEE Commun. Surveys Tuts.*, vol. 24, no. 1, pp. 611–652, Dec. 2022.

[4] X. You, C.-X. Wang, J. Huang, X. Gao, Z. Zhang, M. Wang, Y. Huang, C. Zhang, Y. Jiang, J. Wang, and M. Zhu, "Towards 6G wireless communication networks: Vision, enabling technologies, and new paradigm shifts," *Sci. China Inf. Sci.*, vol. 64, no. 1, pp. 5–78, Jan. 2021.

[5] H. He, X. Yu, J. Zhang, S. Song, and K. B. Letaief, "Cell-free massive MIMO for 6G wireless communication networks," *J. Commun. Inf. Netw.*, vol. 6, no. 4, pp. 321–335, Dec. 2021.

[6] K. Samdanis and T. Taleb, "The road beyond 5G: A vision and insight of the key technologies," *IEEE Netw.*, vol. 34, no. 2, pp. 135–141, Mar. 2020.

[7] H. Q. Ngo, L.-N. Tran, T. Q. Duong, M. Matthaiou, and E. G. Larsson, "On the total energy efficiency of cell-free massive MIMO," *IEEE Trans. Green Commun. Netw.*, vol. 2, no. 1, pp. 25–39, Mar. 2018.

[8] Y. Li and G. A. A. Baduge, "NOMA-aided cell-free massive MIMO systems," *IEEE Wireless Commun. Lett.*, vol. 7, no. 6, pp. 950–953, Dec. 2018.

[9] M. Bashar, K. Cumanan, A. G. Burr, H. Q. Ngo, L. Hanzo, and P. Xiao, "On the performance of cell-free massive MIMO relying on adaptive NOMA/OMA mode-switching," *IEEE Trans. Commun.*, vol. 68, no. 2, pp. 792–810, Feb. 2020.

[10] J. Zhang, J. Fan, J. Zhang, D. W. K. Ng, Q. Sun, and B. Ai, "Performance analysis and optimization of NOMA-based cell-free massive MIMO for IoT," *IEEE Internet Things J.*, vol. 9, no. 12, pp. 9625–9639, Jun. 2022.

[11] J. Zheng, J. Zhang, and B. Ai, "UAV communications with WPT-aided cell-free massive MIMO systems," *IEEE J. Sel. Areas Commun.*, vol. 39, no. 10, pp. 3114–3128, Oct. 2021.

[12] V. Tentu, E. Sharma, D. N. Amudala, and R. Budhiraja, "UAV-enabled hardware-impaired spatially correlated cell-free massive MIMO systems: Analysis and energy efficiency optimization," *IEEE Trans. Commun.*, vol. 70, no. 4, pp. 2722–2741, Apr. 2022.

[13] X. Zhang, D. Guo, K. An, and B. Zhang, "Secure communications over cell-free massive MIMO networks with hardware impairments," *IEEE Syst. J.*, vol. 14, no. 2, pp. 1909–1920, Jun. 2020.

[14] T. M. Hoang, H. Q. Ngo, T. Q. Duong, H. D. Tuan, and A. Marshall, "Cell-free massive MIMO networks: Optimal power control against active eavesdropping," *IEEE Trans. Commun.*, vol. 66, no. 10, pp. 4724–4737, Oct. 2018.

[15] T. Van Chien, E. Bjornson, and E. G. Larsson, "Joint power allocation and load balancing optimization for energy-efficient cell-free massive MIMO networks," *IEEE Trans. Wireless Commun.*, vol. 19, no. 10, pp. 6798–6812, Oct. 2020.

[16] T. H. Nguyen, T. K. Nguyen, H. D. Han, and V. D. Nguyen, "Optimal power control and load balancing for uplink cell-free multi-user massive MIMO," *IEEE Access*, vol. 6, pp. 14462–14473, 2018.

[17] L. Cantor, "Global internet phenomena report 2022," Sandvine, Waterloo, ON, Canada, Tech. Rep., Jan. 2022.

[18] D. Lecompte and F. Gabin, "Evolved multimedia broadcast/multicast service (eMBMS) in LTE-advanced: Overview and Rel-11 enhancements," *IEEE Commun. Mag.*, vol. 50, no. 11, pp. 68–74, Nov. 2012.

[19] T. X. Doan, H. Q. Ngo, T. Q. Duong, and K. Tourki, "On the performance of multigroup multicast cell-free massive MIMO," *IEEE Commun. Lett.*, vol. 21, no. 12, pp. 2642–2645, Dec. 2017.

[20] X. Zhang, D. Guo, K. An, Z. Ding, and B. Zhang, "Secrecy analysis and active pilot spoofing attack detection for multigroup multicasting cell-free massive MIMO systems," *IEEE Access*, vol. 7, pp. 57332–57340, 2019.

[21] M. Zhou, Y. Zhang, X. Qiao, M. Xie, L. Yang, and H. Zhu, "Multigroup multicast downlink cell-free massive MIMO systems with multiantenna users and low-resolution ADCs/DACs," *IEEE Syst. J.*, vol. 16, no. 3, pp. 3578–3589, Sep. 2022.

[22] J. Li, Q. Pan, Z. Wu, P. Zhu, D. Wang, and X. You, "Spectral efficiency of unicast and multigroup multicast transmission in cell-free distributed massive MIMO systems," *IEEE Trans. Veh. Technol.*, early access, Aug. 2, 2022, doi: 10.1109/TVT.2022.3195776.

[23] S. Zhang, J. Liu, H. Guo, M. Qi, and N. Kato, "Envisioning device-to-device communications in 6G," *IEEE Netw.*, vol. 34, no. 3, pp. 86–91, Jun. 2020.

[24] A. Asadi, Q. Wang, and V. Mancuso, "A survey on device-to-device communication in cellular networks," *IEEE Commun. Surveys Tuts.*, vol. 16, no. 4, pp. 1801–1819, Nov. 2014.

[25] T. Yoon, T. H. Nguyen, X. T. Nguyen, D. Yoo, B. Jang, and V. D. Nguyen, "Resource allocation for NOMA-based D2D systems coexisting with cellular networks," *IEEE Access*, vol. 6, pp. 66293–66304, 2018.

[26] Y.-D. Lin and Y.-C. Hsu, "Multihop cellular: A new architecture for wireless communications," in *Proc. 19th Annu. Joint Conf. IEEE Comput. Commun. Soc. (INFOCOM)*, vol. 3, Mar. 2000, pp. 1273–1282.

[27] K. Doppler, M. Rinne, C. Wijting, C. B. Ribeiro, and K. Hugl, "Device-to-device communication as an underlay to LTE-advanced networks," *IEEE Commun. Mag.*, vol. 47, no. 12, pp. 42–49, Dec. 2009.

[28] A. He, L. Wang, Y. Chen, K.-K. Wong, and M. Elkashlan, "Spectral and energy efficiency of uplink D2D underlaid massive MIMO cellular networks," *IEEE Trans. Commun.*, vol. 65, no. 9, pp. 3780–3793, Sep. 2017.

[29] X. Lin, R. W. Heath, Jr., and J. G. Andrews, "The interplay between massive MIMO and underlaid D2D networking," *IEEE Trans. Wireless Commun.*, vol. 14, no. 6, pp. 3337–3351, Jun. 2015.

[30] M. Xie, X. Jia, M. Zhou, and L. Yang, "Study on energy efficiency of D2D underlay massive MIMO networks with power beacons," in *Proc. 8th Int. Conf. Wireless Commun. Signal Process. (WCSP)*, Oct. 2016, pp. 1–5.

[31] H. Masoumi, M. J. Emadi, and S. Buzzi, "Coexistence of D2D communications and cell-free massive MIMO systems with low resolution ADC for improved throughput in beyond-5G networks," *IEEE Trans. Commun.*, vol. 70, no. 2, pp. 999–1013, Feb. 2022.

[32] X. Qiao, Y. Zhang, M. Zhou, L. Yang, and H. Zhu, "Downlink achievable rate of D2D underlaid cell-free massive MIMO systems with low-resolution DACs," *IEEE Syst. J.*, vol. 16, no. 3, pp. 3855–3866, Sep. 2021.

[33] B. Zhou, H. Hu, S. Q. Huang, and H. H. Chen, "Intracluster device-to-device relay algorithm with optimal resource utilization," *IEEE Trans. Veh. Technol.*, vol. 62, no. 5, pp. 2315–2326, Jun. 2013.

[34] E. Björnson, M. Matthaiou, D. W. K. Ng, H. Yang, and D. J. Love, "Prospective multiple antenna technologies for beyond 5G," *IEEE J. Sel. Areas Commun.*, vol. 38, no. 8, pp. 1637–1660, Aug. 2020.

[35] S. Buzzi, C. D'Andrea, A. Zappone, and C. D'Elia, "User-centric 5G cellular networks: Resource allocation and comparison with the cell-free massive MIMO approach," *IEEE Trans. Wireless Commun.*, vol. 19, no. 2, pp. 1250–1264, Feb. 2020.

[36] X. Hu, C. Zhong, X. Chen, W. Xu, H. Lin, and Z. Zhang, "Cell-free massive MIMO systems with low resolution ADCs," *IEEE Trans. Commun.*, vol. 67, no. 10, pp. 6844–6857, Oct. 2019.

[37] T. L. Marzetta, E. G. Larsson, H. Yang, and H. Q. Ngo, *Fundamentals Massive MIMO*. Cambridge, U.K.: Cambridge Univ. Press, 2016.

[38] T. C. Mai, H. Q. Ngo, and T. Q. Duong, "Downlink spectral efficiency of cell-free massive MIMO systems with multi-antenna users," *IEEE Trans. Commun.*, vol. 68, no. 8, pp. 4803–4815, Aug. 2020.
[39] H. Cramer, *Random Variables and Probability Distributions*. Cambridge, U.K.: Cambridge Univ. Press, 1970.

JINWEN LI received the B.E. degree in electronic and information engineering from Guangdong Ocean University, Zhanjiang, China, in 2021. He is currently pursuing the M.S. degree with the Anhui University of Science and Technology, Huainan, China. His current research interests include cell-free massive MIMO and artificial intelligence.

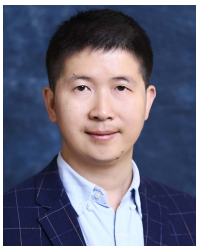

ANPING WAN received the B.E. degree in traffic equipment information engineering from Central South University, Changsha, China, in 2007, and the M.S. and Ph.D. degrees in thermal engineering from Zhejiang University, Hangzhou, China, in 2010 and 2014, respectively. He used to work as a Postdoctoral Fellow at the Mechanical Engineering College, Institute of Mechanical Manufacturing and Automation, Zhejiang University, from 2014 to 2016, where he was a Postdoctoral Fellow at the Mechanical Engineering College, Computer Science and Technology Institute, from 2016 to 2019. He is currently an Associate Professor with Zhejiang University City College, Hangzhou. His research interests include mechanical and energy engineering with a special interests of fault diagnosis and health management of complex equipment.

MENG ZHOU received the Ph.D. degree from the College of Communication and Information Engineering, Nanjing University of Posts and Telecommunications, Nanjing, China, in 2021. He is currently a Postdoctoral Fellow with Zhejiang University, Hangzhou, China. His research interests include wireless communications, with a special interest of cell-free massive MIMO, D2D communication, physical layer security, and HetNets.

JIANTAO YUAN (Member, IEEE) received the B.E. degree in electronic and information engineering from Dalian University, Dalian, China, in 2009, the M.S. degree in signal and information processing from The First Research Institute of Telecommunications Technology, Shanghai, China, in 2012, and the Ph.D. degree from the College of Information Science and Electrical Engineering, Zhejiang University, Hangzhou, China. He was with Datang Mobile Communication Equipment Company Ltd., Shanghai, from 2012 to 2013, where he was involved in LTE network planning and optimization. He used to work as a Postdoctoral Fellow at the Ocean College, Institute of Ocean Sensing and Networking, Zhejiang University, from 2019 to 2021. He is currently working with the School of Information and Electrical Engineering, Zhejiang University City College, Hangzhou. His research interests include cell-free massive MIMO, cross-layer protocol design, 5G new-radio-based access to unlicensed spectrum (NR-U), and ultra-reliable low latency communications (uRLLC).

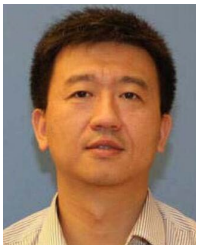

RUI YIN (Senior Member, IEEE) received the B.S. degree in computer engineering from Yanbian University, China, in 2001, the M.S. degree in computer engineering from the University of KwaZulu-Natal, Durban, South Africa, in 2006, and the Ph.D. degree in information and electronic engineering from Zhejiang University, in 2011.

From March 2011 to June 2013, he was a Research Fellow with the Department of Information and Electronic Engineering, Zhejiang University, China. He is currently a Professor with the School of Information and Electrical Engineering, Zhejiang University City College, China, and a joint Honorary Research Fellow with the School of Electrical, Electronic, and Computer Engineering, University of KwaZulu-Natal. His research interests include radio resource management in LTE unlicensed, millimeter wave cellular wireless networks, HetNet, cooperative communications, massive MIMO, optimization theory, game theory, and information theory. He regularly serves as the Technical Program Committee (TPC) boards of the prominent IEEE conferences, such as ICC, GLOBECOM, and PIMRC and the chair some of their technical sessions.

LONGXIANG YANG is currently with the College of Communications and Information Engineering, Nanjing University of Posts and Telecommunications (NJUPT), Nanjing, China, where he is also a Full Professor and a Doctoral Supervisor. His research interests include the broad area of wireless networks, cooperative communications, and signal processing of communications. He has fulfilled multiple National Natural Science Foundations of People's Republic of China.